SISSA - SCUOLA
INTERNAZIONALE
SUPERIORE
DI STUDI AVANZATI
TRIESTE
Strada Costiera 11

ISAS - INTERNATIONAL SCHOOL FOR ADVANCED STUDIES

ATTESTATO DI RICERCA

"MAGISTER PHILOSOPHIAE"

STARBURST GALAXIES

CANDIDATE:

XU Cong

SUPERVISOR:

Prof. G. DE ZOTTI

Academic Year 1985/86

TRIESTE

STARBURST GALAXIES

CANDIDATE:
XU CONG

SUPERVISOR:
PROF. G. DE ZOTTI

A THESIS SUBMITTED FOR THE ATTAINMENT OF
THE DEGREE OF PHILOSOPHY MAGISTER AT THE
S.I.S.S.A. TRIESTE IN ITALY

OCTOBER 1986

Acknowlegement

My gratitude is duo to Prof. G. De Zotti, my superviser, for introducing me to this very interesting field, and for his very careful and enthusiatic guidance.

I would like to thank Prof. L. Danese for many very useful discussions and comments on the work of this thesis.

I am also grateful to Dr. A. Franceschini for his kind helps in the work as well as in the preparation of this thesis.

CONTENTS

STARBURST GALAXIES

CHAPTER I. Introduction

Starburst galaxies are galaxies containing intense formation of massive stars (star formation rates may be tens or even hundreds times larger than normal), which may last 10**7--10**8 years (Huchra 1976b; Biermann and Fricke 1977; Larson and Tinsley 1977; Rieke et al 1980). They may be identified through their bright sharp emission lines characteristic of HII regions. They usually have ultraviolet excesses, radio and X-ray emissions larger than those of normal galaxies, and strong mid- and far-infrared radiations with large Lir/Lop ratios.

Starburst galaxies have been selected mainly in 3 ways: optical photometry; far-infrared observations; and studies of morphologically peculiar objects.

Most optically selected starburst galaxies come from the Markarian lists of unusually blue galaxies (Markarian 1967, 1969a, 1969b; Markarian and Lipovetsky 1971, 1972, 1973, 1974, 1976a, 1976b; Markarian, Lipovetsky and Stepanyan 1977a, 1977b, 1979a, 1979b, 1981).

Standard IR selected starburst galaxies are some nearby galaxies, such as M82 and NGC253 (Rieke and Lebofsky 1979; Rieke et al 1980; Jones and Rodrigues-Espinosa 1984). They are characterized by mid- and far-infrared excesses, attributed to reradiation by dust of ultraviolet radiation from hot young stars and by several IR emission features in the infrared spectrum (Gillett et al 1975; Russell, Soifer, and Merill 1977; Willner et al 1977), which do not appear in the spectra of normal galaxies (Roche and Aitken 1985 and references therein). The IRAS satellite demonstrated that far-IR observations are a very powerful tool for discovering objects of this class.

Galaxies with peculiar or disturbed morphology due to ongoing or recent interaction are always found to be starburst galaxies (Larson and Tinsley 1978).

Starburst galaxies are relatively common among field galaxies: more than 6% of field galaxies brighter than M_B =-15 have evidences of starbursts (Huchra 1977). A large fraction of them (30-50%) have this phenomenon confined to a nucleus a few hundreds parsecs in diameter (Balzano 1983). The starburst nuclei are currently of great interest, since they may

provide insights into the nature and evolution of active galactic nuclei (AGNs, i.e. Seyferts, QSOs, BL Lac objects). If the primary source of the nonthermal emission of AGNs is accretion onto a massive compact object, then the nuclear starburst phenomenon constitutes an ideal situation for the development of active galaxies, since when the burst of star formation is completed, many massive star remnants will be confined to the nuclear region.

Starburst galaxies are heavily represented among the bright extragalactic infrared sources (such as IRAS selected sources). They are also likely to play an important role in the interpretation of very-deep VLA count of extragalactic radio sources (Windhorst et al 1985), and may also be significant contributors to the X-ray background (Weedman 1985).

In addition, the study of evolution of starburst galaxies will provide us with interesting clues on such important subjects as galaxy formation and evolution, and occurrence of the QSO phenomenon.

In Chapter II of this thesis, the classification of starburst galaxies is given. Chapter III describes their observational properties. Chapter IV studies their behaviour as a population. Chapter V discusses

the correlation between starbursts and galactic interactions, and Chapter VI deals with the relation with other classes of active galaxies.

CHAPTER II. Classification of Starburst Galaxies

Depending on their morphological appearance, i.e. on the scale and location of bursts of star formation, starburst galaxies can be classified into 3 subclasses: galaxies with starburst nuclei, blue compact galaxies, and galaxies with giant HII regions outside the nuclei (Sramek and Weedman 1985).

Markarian (1967,1972) divided the objects in his lists into 2 classes--"stellar" and "diffuse"--based on their appearances on prism survey plates. The majority of non-Seyfert "stellar" Markarian objects turn out to be galaxies with starburst nuclei (Balzano 1983). The typical dimension of starburst nuclei is a few hundreds parsecs, while the involved mass is estimated to be around 10**8 M⊙. Starburst nuclei occur much more frequently in spiral galaxies; their distribution along the Hubble sequence peaks at Sb (Figure 2.1, Balzano 1983), while the non-Seyfert Markarian galaxies on the whole have a nearly uniform distribution. Balzano (1983) estimated that about 3% of field galaxies with $-17.5 > M_B > -22.5$ have starburst nuclei.

Blue compact galaxies are usually irregular dwarf galaxies ($M_B > -18$). Their structure is clumpy and

shows a lack of a central condensation. They are very blue (most of them have U-B < 0) and have HII-region-like emission line spectra. It is obvious that rapid star formation occurs simultaneously in the entire structure of these galaxies. Based on a near-infrared study of blue compact dwarf galaxies, Thuan (1983) pointed out that generally blue compact galaxies are not young galaxies (no one in his sample of 36 galaxies is young in the sense that more than 50% of its stars formed in the most recent starburst). The newly formed stars in these galaxies are superposed to an old stellar background.

Some nearby galaxies, such as M31, M101, have been found having very large HII regions outside their central region. The conspicuous rapid star formation in these giant HII regions could be considered as a localized starburst.

In the following, I will be primarily dealing with galaxies with starburst nuclei because of the more obvious correlation between this subset and other classes of AGNs.

CHAPTER III. Observational Properties of Starburst Galaxies

3.1 Optical Photometry

Starburst galaxies were discovered as an independent group first from a photometric analysis of blue galaxies (Markarian 1967,1972; Weedman 1973; Huchra 1977a, 1977b) and peculiar galaxies (Sargent and Searle 1970; Searle and Sargent 1972; Larson and Tinsley 1978).

Markarian (1972) pointed out that the objects in his survey formed a new category of galaxies with the spectral characteristics of stars in the classes A and F, with the blue light in the central parts, while the normal galaxies usually have red light and spectral characteristics of stars in the classes of G and K (Markarian et al 1965,1966; De Vaucouleurs 1961, Morgan and Mayall 1963). He concluded that the diffuse galaxies in his lists represented associations of stars and gas, but the "stellar" objects-- galaxies with bright nuclei--are closely related to nonthermal sources. The latter conclusion has been proved to be wrong by other authors (Weedman 1973; Huchra 1976a,b).

Weedman (1973) was the first one pointing out,

through a photometric study, that the non-Seyfert Markarian galaxies are intrinsically different from Seyfert galaxies. He found that Markarian Seyferts and Markarian non-Seyfert galaxies formed two separated distributions in the U-B vs B-V diagram (Figure 3.1.1). He suggested that different energy-input mechanisms were operating in Seyfert and non-Seyfert blue galaxies, and that the strong nonthermal activity did not occur in the non-Seyfert galaxies.

Huchra (1977a) conducted a comprehensive UBV photometric study of non-Seyfert Markarian galaxies. In his "complete photometric sample", there are 91 Markarian galaxies with apparent photographic magnitude $\leq$ 16.0 and absolute magnitude $>$ -20.35. After correcting the photometric data for absorption within our own Galaxy and for the aperture effect, he found that the Markarian galaxies (name given by Huchra to non-Seyfert galaxies in Markarian lists) locate, in the U-B vs B-V diagram, in a region bluer than that occupied by ordinary field galaxies and have a larger dispersion (Figure 3.1.2). When Markarians are classified by their morphological type, he found that early type (elliptical, SO, Sa, Sb) Markarians fall in the same region of the two colors diagram as field galaxies of the same morphological types, though they

always appear in the blue end. For late Hubble types (Sbc--Im), Markarian galaxies locate in a region bluer than late type field galaxies, but a significant overlap occurs.

Huchra (1977b) calculated 3 classes of evolutionary models for galactic colors: old galaxy models, young galaxy models, and so called "composite" galaxy models -- an old galaxy (--10**10 yrs old) plus a burst of recent star formation. He found that the composite models could explain U-B vs B-V diagram of Markarians best.

Figure 3.1.3 shows the loci in two colors plane for simple two-components systems composed of different concentrations of bursts superposed on old galaxies. Curves 1,2 are a star burst with a duration of 2.5 10**7 years and an initial mass function (IMF) with slope a1=1.35 superposed on old galaxies with a same Salpeter IMF (a0=2.35) but different star formation decay time-scales $t_0 = 1.5 \times 10^9$ yrs , and $t_0 = 5 \times 10^9$ yrs respectively. On curve 3, both starburst and old galaxy have a Salpeter IMF. The bursts are the bluest points on the curves. The underlying galaxies are the reddest. Intermediate points correspond to system with varying contributions of the burst to the V band. With

the Salpeter IMF (a1=2.35) less than 1% of galaxy mass is needed to produce a burst with the V band light equal to the underlying galaxy. For a burst with a1=1.35, this fraction drops to less than 0.1%.

In Figure 3.1.4 we see the color-color evolution of two representative composite models. In both cases the burst has a1=1.35 and a duration of 2.5 10**7 years. Its colors at maximum are U-B=-0.91 and B-V=-0.09, and its strength has been adjusted to be 50% of V light at its maximum light. The evolution track is 10**8 years long, with ticks on 10**7 years time scale. The loci of the color-color track for composite models with the same underlying galaxy but different IMFs and durations of bursts are similar: only the time scales along the tracks change. Models with lower a1's for the burst decay more rapidly.

An important investigation of the photometric properties of peculiar galaxies, showing bluer colors and larger dispersion in two color diagram than field galaxies (Figure 3.1.5), is due to Larson and Tinsley (1978). Using a technique similar to Huchra's (1977b), they found that peculiar galaxies too definitely require bursts of star formation to account for their continuum colors. Since the majority of peculiar

galaxies are in interacting systems (Arp 1966), the similarity in the photometric behavior of peculiar galaxies and Markarian galaxies suggests a correlation between interactions and starbursts. This point will be discussed further in chapter V.

3.2 EMISSION LINE SPECTRUM

Starburst galaxies are characterized by their HII-region-like spectrum, due to the significant condensation of bright young O,B stars in them. Baldwin, Phillips, and Terlevich (1981) constructed two dimensional classification schemes which separate emission-line objects characterized by different ionization mechanisms. Using one of their schemes exploiting the line ratios [NII] 6584 : Hα and [OIII] 5007 : Hβ, Balzano (1983) showed that most galaxies with starburst nuclei locate in the box of HII regions (Figure 3.2.1). Their excitation levels are low. They generally have [OIII] 5007:Hβ < 3 (Shuder et al 1981) and 0.2 < [NII]6584:Hα < 0.5.

The emission lines of starburst galaxies are very sharp and symmetric (with approximate Gaussian profiles). Usually they have a full width at half-maximum (FWHM) less than 250 km/sec. Feldman et

al (1982) gave a median FWHM of 160 km/sec for starburst nuclei. The median velocity dispersion a (a=FWHM/2.35) estimated from this mean FWHM is 68 km/sec. Comparing with the median velocity dispersion of normal spiral nuclei (Whitmore, Kirshner, and Schechter 1979; Whitmore and Kirshner 1981), which is 150 km/sec, it appears that the burst and the accompanying young star population are not in dynamical equilibrium with the original nuclear contents.

Huchra (1977a) examined the correlations between some emission line properties and photometric properties. Table 3.2.1 is adapted from his Table 9. It gives the linear correlation coefficient R (Bevington 1969) and the parameters of linear fits for pairs of quantities whose correlation probability exceed 95%. $W(H_\beta)$ is the H_β equivalent width in emssion, E is the excitation parameter (E=[OIII] 5007/H_β), USB is the U band surface brightness, and BSB is the B band surface brightness. Most of these correlations are expected. The bluer or "hotter" objects have stronger emission lines and higher excitation. Excitation is correlated more strongly with blue surface brightness than with ultraviolet surface brightness. There is less correlation of H with B-V than with U-B. This is probably caused by the

much smaller range in B-V colors plus the fact that the Balmer continuum emission contributes to the U-B color, whereas $H\beta$ and the [OIII] lines lie between B and V in low redshift galaxies.

3.3 Near Infrared

It has long been known that QSOs and Seyferts show near infrared excess, i.e. a large J-K (Rieke and Low 1972; Rieke and Lebofsky 1979; Balzano and Weedman 1981). Do starburst galaxies have similar properties? The answer is no.

Balzano and Weedman (1981) presented JHK photometry of 107 nuclei of galaxies. Among them, 44 are non-Seyfert Markarians, 33 are Seyfert galaxies, and other 33 are NGC galaxies with bright and compact nuclei regardless of any spectroscopic or photometric properties. In 44 non-Seyfert Markarians (4 of them are binary systems), only 5 (i.e. ~10%) have J-K>1.2. Figure 3.3.1 shows a U-B vs J-K diagram for starburst nuclei and Seyfert galaxies. It can be seen that Seyferts have much redder J-K than starburst nuclei. The mean J-K of starburst nuclei obtained by Balzano and Weedman (1981) is $1.02\pm.12$, while the mean J-K of Seyferts is 1.56.

Balzano (1983) found that the distribution of J-K and H-K colors of starburst nuclei is very similar to that of nuclei of bright NGC galaxies (Table 3.3.1, Fig.3.3.2), the mean colors <J-K> and <H-K> are also close to those found for normal E and SO galaxies (Frogel et al 1978). She concluded that for starburst nuclei, the near infrared light comes primarily from the cool, old star population, as is the case for normal galaxies.

However, from Figure 3.3.2, especially from the distribution of J-K, we find a slightly larger dispersion in starburst nuclei than in normal nuclei. A similar situation was found by Cutri and McAlary (1985) for interacting galaxies. This can be explained as a weak influence of the starburst activity on the near infrared properties of nuclei, due either to radiation from dust, or to radiation from red supergiants .

A near infrared study of blue compact dwarf galaxies was carried out by Thuan (1983). A mean <J-K> of 0.83±.16 was found, which is close to the mean <J-K> obtained by Aaronson et al (1978) of 0.9±0.08 for Scd-Sd galaxies. Thuan (1983) concluded that the distribution of compact blue dwarf galaxies in the J-H

vs H-K diagram (Figure 3.3.3) can be explained by assuming that near infrared fluxes come primarily from an old population of K and M giants. He found that a model combining an old galaxy with a burst of star formation can explain the U-B vs V-K diagram very well.

3.4 Mid- and Far-infrared

In this band, the normal stellar contribution is very weak. The main sources of mid- and far- infrared emission are warm dust and/or nonthermal sources. Three processes may be relevant: a. reradiation by dust heated by hot stars; b. reradiation by dust heated by nonthermal sources; c. direct emission from nonthermal sources. In the cases of normal galaxies and starburst galaxies, where the nonthermal sources are weak or absent, only reradiation by dust heated by very hot young stars is important. Thus the mid- and far- infrared behavior of galaxies is a good indicator of starburst activity (Wynn-Williams 1982; de Jong et al 1984; Lonsdale et al 1984).

Jura (1982) has predicted the appearance of spiral galaxies in the infrared using a simple model where star light is thermalized in the disk of a galaxy and the dust is uniformly mixed with stars. This model

predicts an effective temperature for IR emssion ~25 K and a ratio $L_{60\mu}/L_B$ of about 0.2 ($L_{60\mu}$ and L_B are calculated from flux(ν)*ν).

De Jong et al (1984) analyzed a sample of bright galaxies drawn from the revised Sharply-Ames Catalogue (Sandage and Tammann 1981), complete to B=13 mag, and found that most of them have Lir/L_B a factor of 2 larger than predicted by Jura (1982) (Figure 3.4.1); the estimated color temperatures are also generally higher. They suggested a two components model to explain this excess. In addition to the interstellar dust distributed through the disk, considered by Jura (1982), they postulated a substantial contribution from dust associated to HII regions and molecular clouds reradiating the light of the most recently born O stars at a temperature of approximately 50 K. When the rate of star formation in a galaxy is high, as is the case in starburst galaxies, the warmer component becomes increasingly more important. Thus the Lir/Lop ratio and the color temperature should both increase with increasing star formation rate, as shown in Fig. 3.4.1.

Lawrence et al (1985) carried out infrared observations (from 1 to 20 microns) of low-level active

galactic nuclei (Seyfert 2s, starbursts, LINERs) in spiral galaxies. They had 6 starburst nuclei in their sample, all of them were found to have an infrared spectrum similar to NGC5461, a prototype extragalactic HII region in the nearby spiral galaxy M101. The very steep N-Q color index (~10--20 microns), corresponding to a spectral index a--3, of NGC5461 is attributed to dust. The flattish JHK colors can be explained by emission from an old stellar population plus recombination radiation. In near infrared, starburst nuclei show some differences with respect to NGC5461 (Fig. 3.4.2), most likely due to the emission from a substantial population of red supergiants, as discussed in the previous section.

Deutsch and Willner (1986) studied the far-infrared behavior of galaxies with starburst nuclei in Balzano's (1983) sample. They found that starburst galaxies are notably more luminous in the far-IR than normal spiral galaxies; the far-IR luminosities are the largest contributors to the total light of them--a mean <Lir/Lop> of 2.45 has been found. The far-infrared, the $H\alpha$, and the blue luminosities are all correlated with one another. The far-infrared emission seems, however, better correlated with the blue than with the $H\alpha$ emission, possibly implying that the dust producing

the far-infrared light is heated predominantly by B rather than by O stars.

A tight correlation between far-IR and radio emissions was found by De Jong et al (1985) for all spiral galaxies.

Since many evidences show that the IR excess is associated with enhanced star formation, some authors (Rieke 1978; Rieke and Lebofsky 1980; Keel 1980; Condon et al 1982; Rudy 1984; Rudy et al 1984; Smith 1985) argued that IR excess is better as a criterion for selecting starburst galaxies than UV excess , because the UV spectrum can be reddened by dust extinction easily. The prototype IR selected starburst galaxy is M82 (Rieke et al 1980). It is a very bright infrared source with a large Lir to Lop ratio: Lir/Lop--4 (Soifer et al 1984), but its optical colors are quite red (U-B=0.38, B-V=0.89, cf. de Vaucouleurs et al 1976). Other examples of IR selected starburst galaxies are NGC253 (Becklin, Fomalont, and Neugebauer 1973; Glass 1973; Rieke and Low 1975; Rieke et al, 1980), and NGC5253 (Moorwood and Glass 1982). Smith (1985) points out that since our knowledge about starburst galaxies comes premarily from blue galaxies, mostly from the Markarian survey, and there is,

correspondingly, a severe bias against objects with dust extinction, our view of their overall properties and of their evolution could be a very distorted one.

3.5 Radio

Starburst galaxies are not very powerful radio sources. From the first 7 Markarian lists (Mk 1--700) 42 galaxies were found having S(6 cm)>30 mJy (Sremak and Tovmassian 1975; Sulentic 1976; Kojoian et al 1980). Ten of them are Seyferts, and 4 are BL Lac objects or possible BL Lacs. Of the remaining 28 non-Seyfert objects, the 15 with morphological classification are all spirals. The mean monochromatic luminosity <L(6 cm)> of the 26 having measured redshifts is 21.17±0.70 W/Hz/ster, significantly higher than that of normal spiral galaxies of similar optical luminosities, but lower than that of giant ellipticals (cf. Ekers 1973).

Using the 5GHz radio observations of Sramek and Tovmassian (1975) together with the UBV data of Weedman (1973), Biermann and Fricke (1977) checked their own starburst model, and found that bursts with duration time 2×10^7 to 8×10^7 yrs, consistently with the results

of Huchra (1977b) and Larson and Tinsley (1978), can explain the $S(5GHz)/L_B$ vs (B-V) diagram of Markarians very well.

Sulentic (1976) found that the optical luminosities and the radio luminosities of Markarian galaxies are fairly well correlated (the correlation coefficient is about 0.7 for a sample containing 36 objects, including 8 Seyferts). This can be understood since the optical emission of starburst galaxies is dominated by very bright O,B stars, while the radio emission is dominated by thermal bremsstrahlung from ionized gas and nonthermal emission from remnants of supernovae; O,B stars, ionized gas and supernova remnants are all related to the star formation rate.

In principle, radio observations alone can specify the initial mass function (IMF) of massive stars in an ongoing starburst. This is because the thermal radio luminosity arises as a consequence of the ionizing flux from these stars, thereby relating to their total mass. The nonthermal luminosity relates instead to the number of supernova remnants, so scales with the number of massive stars. Knowing the total mass and the total number of massive stars within a given range specifies the shape of any IMF that is a

power law. In this way, Sramek and Weedman (1986) studied the IMFs for their mixed sample, which consists of starburst nuclei, blue compact galaxies, and giant HII regions. They found , for starburst nuclei, the IMF of the ongoing starburst is a conventional power law (a=2.5), but blue compact galaxies and giant HII regions show a deficiency of supernova remnants.

Twenty one cm neutral hydrogen studies by Bottinelli et al (1973) and Bottinelli et al (1975) showed that Markarian galaxies contained neutral hydrogen in the range of 10**7÷10**10 M⊙, corresponding to a mass fraction of a few percent.

3.6 X-ray

In the X-ray band, starburst galaxies are usually brighter than normal galaxies, but fainter than Seyfert galaxies. Fabbiano, Feigelson and Zamorani (1982) presented X-ray (0.5 to 3 KeV) observations of a sample of 33 peculiar galaxies. There is no uniform, well defined selection criterion for this sample, but most galaxies are in the Arp's catalogue (Arp 1966), and many of them lie in groups and interacting pairs. In the U-B vs B-V diagram, these galaxies are located in the same region of Markarian galaxies (Huchra 1977a),

so they are believed to be starburst galaxies. 13 galaxies were detected at 3σ level with soft X-ray fluxes in the range (2÷17)*10**-13 erg/cm**2/sec. The corresponding luminosities range from 10**39 to 2.3*10**42 erg/sec. The galaxies with higher photon counts show evidences of extended or multiple emission regions, so X-ray emission from these galaxies can not be explained by a single nuclear emission, like in the case of Seyferts. Population I binary X-ray sources and young supernova remnants are suggested to be the most important contributors. Since there are more OB stars (~10**5) in starburst galaxies (Benvenuti et al 1979) than in normal galaxies (e.g. in our own Galaxy, there are ~10**4 OB stars [van den Heuvel 1980]), so more X-ray binaries exist there. Also the supernova explosion rate is higher in starburst galaxies. A SN rate of ~0.2/yr and 200 X-ray binaries will produce X-ray luminosity ~10**40÷42 erg/sec (while in our own Galaxy, the SN rate is ~0.05/yr [Clerk and Stephonson 1982], thare are ~20 X-ray binaries [van der Henvel 1980]). Fabbiano et al (1982) found that the X-ray luminosity is correlated with radio luminosity and optical luminosity. The correlation is stronger with radio luminosity (~7σ level) than with optical luminosity (~3σ level).

CHAPTER IV. Populational Behaviour and Luminosity Functions

4.1 Review

The luminosity function is defined as the number density of sources as a function of their absolute luminosity. As already mentioned, the Markarian survey is the main source of starburst galaxies. Actually, it is widely held that most non-Seyfert Markarians belong to this category. Several estimates of the optical luminosity function of Markarian galaxies are already in the literature (Huchra and Sargent 1973; Huchra 1977a; Balzano 1983).

The best estimate, so far, is due to Huchra (1977a). It is based on 327 galaxies (Seyferts included) with $m_B \leq 15.5$ in the first seven Markarian lists. Absorption corrections and K corrections were neglected. A correction for completeness estimated from an analysis of <V/Vm> as a function of apparent magnitude (Huchra and Sargent 1973) was applied. Fig.4.1.1 shows Huchra's luminosity function compared with the luminosity functions of field galaxies (Christensen 1975) and of Markarian Seyferts. He concluded that Markarians represent approximately 6% of

the field galaxies between M_B=-22 and -15, and this fraction rises at high luminosities.

It is possible now to considerably improve over Huchra's (1977) results in several respects. Making use of all 15 Markarian lists we may pull together a sample of size comparable to Huchra's, still confining ourselves to a bright enough limiting magnitude (m_B =14.5) for completeness to be ensured. In addition, redshift measurements are now available for all objects of our sample (while ~25% of galaxies were rejected by Huchra because they lacked redshifts). Also all but two of our objects have Zwicky magnitudes, which are considerably more accurate than Markarian's estimates, while Zwicky magnitudes are available only for ~50% of objects down to 15.5 magnitude.

Moreover, redshift independent distance estimates, mainly based on the Tully-Fisher (1977) relation, can be found in the published literature for the majority of nearby galaxies ($z \leq 0.007$) whose measured redshifts may have a substantial, or even a dominant, non-Hubble component. Further refinements over previous studies include a careful definition of the mean surface density of Markarian galaxies brighter than m_B=14.5 (allowing for inhomogeneities both in the

sky coverage of the Markarian survey, and in the true spatial distribution of the objects), corrections for errors on magnitudes and for the effect of binning.

Using the IRAS data for objects in our sample, we also constructed a bivariate (optical--IR) luminosity function of non-Seyfert Markarian galaxies. We found that these objects can account only for less than one third of bright IRAS sources. This conclusion disagrees with that of Soifer et al (1986); the reason for the discrepancy is discussed in Section 8, where we also examine the implications of our results.

The population behavior of starburst galaxies is also of interest in other bands. Windhorst et al (1985) found, from their deep 1.4GHz radio survey and multicolor studies of week radio galaxies, that below S(1.4GHz) ~10mJy, a blue radio galaxy population becomes increasingly important, to the point that below 3 mJy 70% of radio sources classified with galaxies belong to this population. The radio to optical luminosity ratios and the frequently peculiar optical morphology, suggestive of interaction and merging, converge in indicating that these radio sources may be associated with starburst galaxies. To account for the observed radio counts, however, we must assume that

they are undergoing cosmological evolution of strength similar to that of QSOs but at much lower luminosities. This would be the first example of strong evolution not directly associated with nuclear emission.

A further important implication would be that, since starburst galaxies are significantly stronger X-ray emitters than normal galaxies (Fabbiano et al 1982), they could also be important contributors to the X-ray background, whose origin is still not well understood.

4.2

OPTICAL AND INFRARED LUMINOSITY FUNCTIONS OF NON-SEYFERT MARKARIAN GALAXIES

I. Definition of the Sample

Our sample was selected from the 15 Markarian lists with following criteria:

<1> $m_B \leq 14.5$

Zwicky magnitudes (Zwicky et al 1961--1968) are available for all galaxies in our sample with only 2 exceptions: Mk789 and Mk1478; Markarian's estimates have been adopted for them.

<2> $|bII| \geq 30^o$; $Dec \geq -2^o$

We have confined ourselves to high galactic latitudes to minimize the uncertainties related to the correction for extinction within our own Galaxy. The limit in declination has an operational meaning: Zwicky magnitudes (which are much more reliable than Markarian's) as well as redshifts (primarily thanks to the CFA survey of Huchra et al (1983)) are available for almost all objects northern of $Dec=-2^o$ and $m_B \leq 14.5$.

<3> Objects classified as QSOs, Seyfert galaxies, and BL Lac objects in Veron and Veron's (1985) catalogue are excluded.

The sample so selected comprises 180 objects, two of them are galactic stars: Mk113 and Mk362. All of the remaining (178) Markarians have redshifts.

II. Determination of the Mean Surface Density

Markarian and his collaborators never stated clearly the boundaries of their survey. Also the coverage of the surveyed region is admittedly far from uniform. Therefore the definition of the mean surface density of the sources brighter than any chosen magnitude limit requires some care. We adopted the following procedure.

First, we divided the region defined by condition <2> into many subregions of equal effective area. The latter has been defined as

$$Qeff=\int 10^{**}(-0.6*A_B)\,dQ \qquad \text{<2.1>}$$

with

$$A_B=0.2*(\csc(bII)-1)$$

<2.2>

to allow for the effect of galactic extinction on the observed counts. Q is the measured solid angle. Eq <2.2> describes reasonably well the mean extinction derived by Burstein and Heiles (1982). Since the apparent magnitude limit is constant, the above operation amounts to dividing our "sample space" into equal volumes. If the objects in our sample are uniformly distributed in space, the distribution of surface densities among subregions should be Poissonian.

The effective area with the boundaries defined by condition <2> is 9699 sq deg. It was divided into 120 subregions plus some residuals with a total effective area of 99 sq deg which do not contain any object. This looked as the finest subdivision with a still reasonable statistic (Fig. 4.2.1). The surface density distribution is showed in Table 4.2.1 and Fig. 4.2.2.

An excess of low surface density regions, corresponding to areas not covered or only poorly covered by the Markarian survey, was indeed expected in Fig.4.2.2. In particular, it is clear from Fig.4.2.1 that the area around the edge has been, in general,

poorly observed. Such area, including one relatively high surface density subregion containing 3 objects, has been correspondingly omitted from further analysis. The objects in the remaining 76 subregions closely follow a Poisson distribution with an average value λ=2.3 (Table 4.2.2, Fig.4.2.3). Although the choice of areas to be omitted is, to some extent, arbitrary, the determination of the mean surface density is obviously independent of it; also, the derived luminosity function is almost insensitive to the particular choice we make since only 11 objects (out of 178) are left aside anyway.

The resulting sample (167 objects) is listed in Table 4.2.3. The reddening within our own galaxy, E(B-V), has been deduced for each object from the maps of Burstein and Heiles (1982). The 11 galaxies in the omitted region are listed in Table 4.2.4. The total effective area of the final sample is 6080 sq deg. The mean surface density of Markarian galaxies brighter than m_B=14.5 is then 0.028/sq deg.

III. Distances of Nearby Galaxies

Redshift distances are obviously unreliable for

nearby objects whose peculiar velocities may easily be comparable to, if not larger than, their Hubble velocity. In view of that, non-redshift distances have been adopted as far as possible. Distances derived from the Tully-Fisher relation (Tully and Fisher 1977) have been found in the literature for 32 nearby galaxies ($z \lesssim 0.007$) in our sample (Table 4.2.5a); the 27 of them which are in groups (Geller and Huchra 1983; Huchtmeier and Richter 1986), have been assigned the distances of the corresponding groups (Giuricin et al 1986). All Tully-Fisher distances have been scaled to an assumed distance of the Virgo cluster of 20 Mpc (Sandage and Tammann 1977). For other 19 nearby galaxies ($z \lesssim 0.007$) in our sample, which have no published Tully-Fisher distance estimates, and also lack enough data to apply the Tully-Fisher method, distances were estimated using the model by Aaronson et al (1982) for the Virgocentric motion (Table 4.2.5b).

All objects which, according to Geller and Huchra (1983) and Huchtmeier and Rechter (1986), are members of the Virgo cluster and of the Ursa major cluster, have been given a distance of 20 Mpc (Sandage and Tammann 1976; Tully and Fisher 1977) irrespective of their redshifts, 3 of them (Mk171, Mk171a, and Mk781) have redshifts $z \gtrsim 0.007$ (Table 4.2.5a).

IV. Completeness and Homogeneity

Using the <V/Vm> method, we checked the completeness of our sample. For a complete sample of uniformly distributed galaxies, we should have <V/Vm>=0.5±1/$\sqrt{12N}$ (Schmidt 1968). Values of <V/Vm> for our final sample and several limiting magnitudes are given in Table 4.2.6. We find <V/Vm> significantly larger than 0.5 at bright magnitudes (m_B(lim)=13, 13.5), as expected since the bright sources were usually excluded from the Markarian lists (Markarian 1967). At m_B (lim)=14.5, the magnitude limit of our sample, <V/Vm>=0.49±0.02. At fainter magnitudes (m_B(lim)=15, 15.5), <V/Vm> drops to values significantly smaller than 0.5, implying that the corresponding samples are incomplete. To check the homogeneity of our sample, we calculated the correlation between apparent magnitudes and absolute magnitudes (Neyman and Scott 1961). Absolute magnitudes were derived according to the formula

$$M_B = m_B - 5*\log(D(\mathrm{Mpc})) - 25 + Ab$$

where Ab=4*E(B-V) is the correction for the absorption in our own galaxy. No K correction or correction for the internal absorption are applied. The Hubble constant H_0 is assumed 50 /(km/sec)/Mpc. We found that

the correlation coefficient is only 0.06; there is thus no indication of any "inhomogeneity".

VI. Optical Luminosity Function

We use the so called "generalized Schmidt estimator" (Felten 1976) to get the first approximation to the optical luminosity function:

$$Gj=\sum_{i=1}^{Nj} 1/V(Mi)$$

where Gj is the estimator of the density of sources in the bin (M_j-0.5 mag, M_j+0.5 mag). Nj is the number of objects in this bin. V(Mi) is the maximum volume within which a galaxy with absolute magnitude Mi (Mj-0.5 mag < Mi <Mj+0.5 mag) can be observed.

$$V(Mi)=Q'/3*dex(0.6*(m(lim)-Mi-25)) \ (Mpc**3)$$

Q' is the effective area covered by our sample

$$Q'=6080 \text{ sq deg}=1.852 \text{ ster}$$

m(lim)=14.5 is the apparent magnitude limit.

To derive the luminosity function (LF), Gj needs two corrections. First, although Zwicky magnitudes are

much more accurate than Markarian's, they still have quite large errors (~0.5 mag, (Fasano 1985)). Second, Gj is actually the integral of the luminosity function between Mj-0.5 and Mj+0.5. When the LF is steep, the corrections for binning may be large (Eddington 1913). To correct for these effects, we have used the iterative technique suggested by Lucy (1974), assuming the errors in Zwicky magnitude to have a gaussian distributio with dispersion σ=0.5. We kept only the first order corrections since the second order corrections were always smaller than statistical errors (Table 4.2.7). The differential LF $Y(M_B)$ is found from

$$Y(M_Bj)=Gj*fj$$

Our estimates of the $Y(M_Bj)$ are given, together with Gj, the correction factors fj, and the statistical errors ej, in Table 4.2.7. ej are calculated using the standard formula for the variance of the generalized Schmidt estimator (Felten 1976):

$$e_j = [\sigma/Y]j=\left[\int_{M_j-0.5}^{M_j+0.5} Y(M_B)/V(M_B)dM_B\right]^{1/2}/\int_{M_j-0.5}^{M_j+0.5} Y(M_B)dM_B$$

In Fig.4.2.4a, we compare our results with Huchra's (1977a). Except at the faint end, where both

we and Huchra have large error bars, our LF is smoother than his. The dip and the bump around M_B=-19 appearing in Huchra's LF are not visible in our LF. At the bright end (M_B ~ -23), our LF is significantly higher than Huchra's (Seyfert excluded).

Among the 167 Markarian galaxies in our sample, only 5, all classified as "stellar" by Markarian and his collaborators, have no emission lines. Of the other 162, 89 were classified as "stellar", 73 as "diffuse". We calculated the luminosity functions for both classes separately. No significant differences are found (Table 4.2.8, Fig.4.2.4b, Fig.4.2.4c).

VII. Far-IR Data

Far infrared fluxes, taken from "Catalogued Galaxies and Quasars bserved in the IRAS Survey", for 157 galaxies of our optical sample are listed in Table 4.2.9 (the remaining 10 lay out of the region surveyed by IRAS). The integrated fluxes between 42.5 microns and 122.5 microns, Fir, are calculated from the formula (Soifer et al 1986)

$$Fir=1.89*10**(-14)*(2.58*f(60\mu)+f(100\mu)) \quad (W/m**2) \qquad <4.1>$$

where f(60μ) and f(100μ) are the flux densities at the two wavelengths, measured in Janskys.

At 60 microns, 129 sources were detected, and other 2 upper limits are available in the IRAS catalog. For the remaining 26, upper limits were derived taking into account the flux limits of the IRAS surveys at 60 microns: 0.5 Jy for the 3 HCON survey, 1.6 Jy for the 2 HCON survey (cf. the IRAS Explanatory Supplement).

Since a completeness analysis is not available for 100 microns observations, upper limits at this wavelength were estimated from those at 60 microns on the basis of the mean flux density ratio, $f(100\mu)/f(60\mu) = 1.843 \pm 0.498$, for objects in our sample detected at both

wavelengths. Indeed, flux densities at 60 microns and 100 microns turn out to be tightly correlated (correlation coefficient r=0.985). Using this ratio and equation <4.1> we estimate the Fir detective limits to be 5.01*10**(-14) W/m**2 and 12.53*10**(-14) for 3 HCON and 2 HCON regions, respectively.

The correlation between optical and IR luminosities has been studied and the bivariate (optical-IR) luminosity function has been derived using the "survival analysis" techniques (Schmitt 1985; Feigelson and Nelson 1985), which allow to fully exploit the information content of upper limits.

VII. Correlation between Optical and IR Emissions

A very strong correlation between optical and IR luminosities of Markarian galaxies has been found (Fig.4.2.5, Fig.4.2.6). The correlation coefficient for monochromatic blue (4400 Å) luminosity and 60 micron luminosity is

r1=0.92

The correlation coefficient for integrated blue and integrated IR (between 42.5 microns and 122.5 microns)

luminosities is

r2=0.89

Rieke and Lebofsky (1986) found a much weaker correlation between optical luminosity and IR luminosity for normal galaxies. There may be at least two reasons for that: first, Markarian galaxies always show bursts of star formation which account for most of their blue luminosities and IR emissions, while older stars may contribute a large fraction of light in normal galaxies. Second, there may be a selection effect in the sense that the Markarian survey may be biased on favor of galaxies with low internal extinction (Smith 1985).

VIII. Infrared Luminosity Function

8.1 Fractional bivariate luminosity function

The fractional bivariate luminosity function f(Lop,Lir) is defined so that f(lop,Lir)dLopdLir gives the probability of finding an object in the interval [Lop, Lop+dLop]*[Lir, Lir+dLir]. We derive f(Lop,Lir) using the following procedure.

Let Ntot is the number of objects in our IR

sample, N_0 the number of objects in the bin $Lop_j \leq Lop < Lop_{j+1}$. The probability, $Pj(Lir_k , Lir_{k+1})$, that these N_0 objects fall in the IR luminosity bin $Lir_k \leq Lir < Lir_{k+1}$ is derived, using the "survival analisis" technique. Then

$$f(Lop,Lir)=(N_0*Pj(Lir_k ,Lir_{k+1})/Ntot)/(dLop*dLir)$$

with

$$dLop=Lop_{j+1} - Lop_j$$

and

$$dLir=Lir_{k+1} - Lir_k$$

8.2 IR luminosity function

Combining the f(Lop,Lir) defined above with the optical luminosity function Y(Lop) derived on section VI, we obtain the IR luminosity function Z(Lir) through the formula

$$Z(Lir)=\int Y(Lop)f(Lop,Lir)\ dLop$$

Table 4.2.10 gives our 60 microns luminosity function, Table 4.2.11 gives the integrated IR luminosity function. They both have a shape very similar to that

of Y(Lop), as a consequence of the very strong correlation between Lop and Lir.

In Figs.4.2.9 and 4.2.10, we compare our IR luminosity function with those of bright IRAS galaxies (Soifer et al 1986) and with the IR luminosity function of field galaxies (Rieke and Lebofsky 1986,RL). The integrated IR luminosity functions of Soifer et al (1986) and RL do agree very well with each other in the region of overlap (after allowance is made for the differences in the definitions of the integrated IR luminosity: Soifer et al neglected the contribution from wavelengths shorter than 42.5 microns which was taken into account by RL). It is clear that the contribution of Markarian galaxies to the far IR local luminosity function of field galaxies is never dominant. The shape of the LF of Markarians is also different from that of galaxies as a whole: the former LF is flatter in the low luminosity region, steeper in the high luminosity region; at the "knee" (Lir=2.2*10**11 Lo), which is also the point where our LF is nearest to that of Soifer et al (1986), the density of Markarian galaxies is about 3 times lower than that of bright IRAS galaxies. The situation is similar for the 60 micron monochromatic LF, where the "knee" is at L(60μ)=10**31.75 erg/sec/Hz. Thus, if our

result are correct, non-Seyfert Markarian galaxies are never the dominant component in any infrared luminosity region. The above conclusion disagrees with the claim of Soifer et al (1986) that the density of bright IRAS sources is similar to that of Markarians. However, they have actually compared the "bolometric" luminosity function of Markarians with the IR luminosity function of bright IRAS sources: i.e. the luminosity function of Markarian galaxies plotted in the Fig.1 of Soifer et al (1986) should be shifted towards lower luminosities by a factor of 3 (according to them, IR light is only one third of the "total" light emitted by Markarian galaxies). Moreover, some apparently misplaced points in the figure concur to give the impression of a good agreement between the densities of Markarian galaxies and of bright IRAS sources.

IX. Further improvement

As discussed in section IV, our sample is apparently complete and homogeous on the whole. However, when we use the <V/Vm> method to check the completeness for each absolute magnitude bin, significant fluctuations are found for M_B >-21 (Table

4.2.12). A likely explanation for them is the inhomogeneity in the galaxy distribution. With the apparent magnitude limit of our sample, 14.5, the largest distance for an object with M_B =-20.5 to be observed is 100 Mpc, which is of the same order of the scale of the largest structures of the universe. As a check of the importance of this effect on the estimate of the local luminosity function, we plan to apply the alternative method suggested by Turner (1979) which allows to derive the shape of the luminosity function independently of the assumption of homogeneity, at the cost of assuming that such shape is the same for galaxies in clusters and in the field.

Furthermore the IRAS catalogue of small extended sources has recently became available to us. This would allow to correct the IRAS fluxes given in the point source catalogue for aperture effects.

We have found that optical selected starburst galaxies are never dominant in any infrared luminosity region. The explanation for this is still open. First of all, we plan to check again our reselt. Should it be confirmed, it may be explained either by the presence of other populations, such as LINERs, which have significant far-IR excess (Lawrence et al 1984);

or by possible selection effects in the Markarian survey (c.f. section 3.4).

We also plan to study other properties, such as radio emission and emission line spectrum, of IR selected objects to investigate the populational content of this category.

CHAPTER V. Galaxy Interactions and Starbursts

Toomre and Toomre (1972) in a classical numerical study of the tidal effects on interactions between pairs of galaxies showed that interactions could result in a redistribution of substantial quantities of material into deeply plunging orbits in galaxies. They suggested that this injection of fresh material deep into the potential well of a galaxy could result in a rapid burst of star formation.

The interaction as a triggering mechanism of star formation was also proposed by several other authors (Searle and Sargent 1972; Searle, Sargent, and Bagnuolo 1973; van den Bergh 1975; Alloin, Bergeron, and Pelat 1973; Huchra 1977a,1977b; Larson and Tinsley 1978). Some statistics available in the literature support this hypothesis, too. Huchra (1977a) found that approximately 20% of Markarian galaxies showed pecularities, indicative of interactions, while the corresponding percentage among NGC galaxies is only~7%. Balzano (1983) found a even higher percentage of starburst nuclei to be in interacting/merging systems: >30%. Direct evidence of burst of star formation triggered by interactions is provided by observations of interacting systems.

Larson and Tinsley (1978) compared the UBV colors of a sample of galaxies, selected from Arp's "Atlas of Peculiar Galaxies" (Arp 1966), with the colors of normal galaxies. They found a significantly larger scatter in the two colors diagram of peculiar galaxies; furthermore, after separating peculiar galaxies into interacting and noninteracting subgroups according to their morphological appearances, they found the scatter to be primarily due to interacting galaxies, while the color-color distribution of non-interacting peculiar galaxies resembles that of normal galaxies (Fig 5.1). They interpreted the scatter as an indication of bursts of star formation.

The spectroscopic study of interacting spiral galaxies by Kennicutt and Keel (1984) and Keel et al (1985) showed that interacting galaxies have: <1> significantly higher levels of emission lines, both in equivalent width and in luminosity; <2> more active and extensive nuclear star formation, irrespective of their Hubble type.

Joseph et al (1984) have performed IR measurements of Arp-atlas interacting pairs, finding strong mid-infrared excesses, indicated by K-L color excesses. They argued strongly that these are

evidences of recent bursts of star formation. They concluded that the interactions were extremely efficient in triggering starbursts, the efficiency apparently approaching 100 %. An interesting result they found is that in no case had both galaxies in an interacting pair shown a K-L excess. They interpreted this fact on the basis of the numerical studies of Toomre and Toomre (1972) and Wright (1972). The maximum tidal disruption and transfer of material occur when the accreting galaxy orbits the "victim" galaxy in the same plane and sense as the rotation of the "victim". Since in any arbitrary interaction between two galaxies conditions close to these are more likely to be met for only one galaxy, it is not surprising that the burst of star formation preferentially appears in one member of the pair.

1 to 10 microns IR observations for a sample of interacting galaxy systems were carried out by Lonsdale, Persson, and Matthews (1984). They found that interacting/merging galaxies as a class have substantially higher infrared luminosities than noninteracting spirals, and this emission is due to ongoing massive star formation, which is about 3 times higher than in normal cases. They also analyzed the results from the IRAS minisurvey, found that a large

fraction, perhaps as much as 30 %, of all far-infrared emission from galaxies arises in starburst triggered by interaction.

X-ray observations of morphologically peculiar galaxies by Fabbiano et al (1982) showed that the detected X-ray fluxes are compatible with the levels of star formation implied by ultraviolet and optical data.

Radio observations of galaxies in pairs and multiple systems (Stocke 1978; Hummel 1981), peculiar galaxies (Heckman 1983), and interacting galaxies (Condon et al 1982), give some further support to the concept of interactions as triggering agent of starbursts. More detailed observations of individual objects at ultraviolet, optical, infrared and radio wavelengths give direct evidences of the interpretation that high rates of star fornation are occuring in some interacting systems, such as NGC7714 (Mk538) (Weedman et al 1981), NGC3690 (Mk171) (Gehrz, Sramek, and Weedman 1983), ZwII40 (Baldwin 1982), NGC5253 (Moorwood and Glass 1982), and M82 (Reike et al 1980).

CHAPTER VI. Relation with other Classes of Active Galaxies

Weedman (1983) investegated the possibility that the remnants of starburst nuclei evolve into Seyfert 1 nuclei and QSOs. Usually starburst nuclei are not larger than a few hundred parsecs in diameter (Balzano 1983); from Hα luminosity, Weedman estimated that a standard starburst would leave more than 2*10**7 M⊙ in compact remnants such as neutron stars or black holes. The few spirals with the most luminous starbursts, L(Hα)>10**42 erg/sec, should have Mr (total mass of remnants) if about 10**9 M⊙. Dynamical processes may then concentrate 10**5 to 10**6 M⊙ of these objects into nuclear volumes with scale size of order 1 pc, and eventually power a Seyfert 1 nucleus by gravitational accretion.

Based on studies of structure and evolution of galactic nuclear discs, which are formed by inflowing stellar mass loss in spherical galaxies, Bailey (1980,1982) built a model to explain how a starburst happens and how a nonthermal nuclear activity follows it. He argued that, only a small amount of interstellar gas is required to give rise to a mass inflow and construct a growing disc. The disc growth,

dominated by infall, continues until the onset of local gravitational instability (Goldreich and Lynden-Bell 1965) close to the center in a region within which the mean mass density q* is less than 10**4 to 10**5 M⊙/pc**3. At this point massive star formation propagates sequentially through the disc (Elmegreen and Lada 1977), leading to a burst of star formation. The viscosity of the disc is greatly enhanced due to a large increase in the rms gas velocity dispersion (turbulent velocity vt >> 1 Km/sec) caused by the starburst, and viscous inflow leads to nuclear activity either by accretion onto a massive black hole, or by the formation of a massive central gas cloud. In the latter case the cloud is presumed to collapse to form either a black hole or a spinar.

Bailey's model is of interest because it not only provides an approach to explain why the starbursts always occur in nuclei of galaxies, but also gives an altenative to interactions as the triggering mechanism: the nuclear interstellar gases may come simply from stellar mass loss. This scenario entails the possibility that non-interating galaxies evolve into stabursts and nonthermal activities, in keeping with the evidence that many starburst galaxies are non-interacting.

Terlevich and Melnick (1985) present another approach on the subject of the relation between Seyfert galaxies and starbursts. They investigated the effect of "warmers" on the evolution of a metal rich giant HII region; "warmers" are massive stars undergoing mass loss at high rate --extreme WC or WO Wolf-Rayet stars-- which can reach an effective temperature > 100,000 K. They found that the spectrum of a sufficiently massive HII region evolves to a Seyfert 2 spectrum and then into a Low Ionization Nuclear Emission-line Region (LINER, Heckman 1980) spectrum.

PLANS OF FUTURE WORK

Straight forward developments of the work discribed here include:

a. A deeper analysis of IRAS data to determine the far infrared spectrum of these sources. Given the steep slope of such spectrum, K-corrections are likely to play a very important role in any attempt to interpret the IRAS counts. A study of correlation of far-IR colors with luminosity will also provide hints on the physics of far-IR emission.

b. A study of radio properties of these sources assesses their contributions to the very deep VLA counts of extragalactic radio sources (Windhorst et al 1985). It is particularly important to analize the latter in view of the possibility that they entail a substantial cosmological evolution of starburst galaxies. Again a comparison with deep IRAS counts will greatly help in assessing this point, given the tight correlation between far-IR and radio luminosities of these sources (de Jong et al 1985).

c. Using the data on X-ray emission of Markarian galaxies we may also give some estimates on their contribution to local luminosity function of X-ray

sources, to the X-ray counts and the X-ray background. These estimates will obviously take into account the constrains on evolution set by radio and IRAS data.

d. Combining the data in radio, IR, optical and X-ray bands we plan to get insights on the internal physics of starburst galaxies.

REFERENCE

Aaronson, M., Huchra, J.P., and Mould, J. 1979, Ap.J. 229, 1.

Aaronson, M., Huchra, J.P., Mould, J., Schechter, P.L., and Tully, R.B. 1982, Ap.J., 258, 64.

Aaronson, M., Huchra, J.P., Mould, J., Tully, R.B., Fisher, J.R., Van Woerden, H., Goss, W.M., Chamaraux, P., Mebold, M., Siegman, B., Berriman, G., and Persson, S.E. 1982, Ap.J. Suppl., 50, 241.

Alloin, D., Bergeron, J., and Pelat, D. 1977, A.Ap., 70, 141.

Arp, H. 1966, "Atlas of Peculiar Galaxies" (Pasadena: California Institute of Technology); also Ap.J. Suppl., 14, No.123.

Bailey, M.E. 1980, M.N.R.A.S., 191, 195

Bailey, M.E. 1982, M.N.R.A.S., 200, 247.

Baldwin, J.A. 1982, M.N.R.A.S., 198, 538.

Baldwin, J.A., Phillips, M.M., and Terlevich, R. 1981, Pub., A.S.P., 93, 5.

Balzano, V.B. 1983, Ap.J., 268, 602.

Balzano, V.A., and Weedman, D.W. Ap.J., 243, 756.

Becklin, E.E., Formalont, E.B., and Neugebauer, G. 1973, Ap.J. (Letters), 181, L27.

Benvenuti, P., Casini, C., and Heidmann, J. 1979, NATURE, 282, 272.

Bevington, P. 1969, "Data Reduction and Error Analysis for the Physical Sciences" (New York: McGraw-Hill).

Biermann, P., and Fricke, K. 1977, A.Ap., 54, 461.

Bottinelli, L., Duflot, R., Gouguenheim, L., and Heidmann, J. 1975, A.Ap., 41, 61.

Bottinelli, L., Gouguenheim, L., and Heidmann, J. 1973, A.Ap., 22, 281.

References

Bottinelli, L., Gouguenheim, L., Patural, G., and de Vaucouleurs, G. 1985, A.Ap. Suppl., 59, 43.

Bottinelli, L., Gouguenheim, L., Patural, G., and Teerikorpi, P. 1986, A.Ap., 156, 157.

Bottinelli, L., Gouguenheim, L., Patural, G., and de Vaucouleurs, G. 1984, A.Ap. Suppl., 56, 381.

Burstein, D., and Heiles, C. 1982, Ap.J. (Letters), 262, L17.

"Cataloged Galaxies and Quasars Observed in the IRAS Survey", 1985, prepared by Carol J. Losdale, G. Helou, J.C. Good, and W.L. Rice (Washington: U.S. Goverment Print Office).

Christenson, C. 1975, A.J., 80, 292.

Clerk, D.H., and Stephenson, F.R. 1982, "Supernovae: A Survey of Current Research"; eds. Rees, M.J. and Stoneham, R.J., p355.

Condon, J.J., Condon, M.A., Gisler, G., Puschell, J.J. 1982, Ap.J., 252, 102.

Cutri, R.M., and McAlary, C.W. 1985, Ap.J., 296, 90.

De Jong, T., Clegg, P.E., Soifer, B.T., and Raimand, E. 1984, Ap.J. (Letters), 278, L67.

De Jong, T., Klein, U., Wielebinski, R., and Wunderlich, E. 1985, A.Ap. (Letters), 147, L9.

Denisyuk, E.K., and Lipovetskii, V.A. 1983, Astrofizica, 19, 229.

Dennefeld, M., and Sevre, F. 1984, A.Ap. Suppl., 57, 253.

De Vaucouleurs, G. 1961, Ap.J. Suppl., 5, 233.

De Vaucouleurs, G., De Vaudouleurs, A., and Corwin, H. G.Jr. 1976, "Second Reference Catalogue of Bright Galaxies", University of Texas Press.

Deutsch, L.K., and Willner, S.P. 1986, Ap.J. (Letters), 306, L11.

Elmegreen, B.G., and Lada, C.J. Ap.J., 241, 552.

Elvis, M., Soltan, A., and Keel, W.C. 1984, Ap.J., 283, 479.

References

Eddington, A.S. 1913, M.N.R.A.S., 73, 359.

Fabbiano, G., Feigelson, E., and Zamorani, G. 1982, Ap.J., 256, 397.

Fasano, G. 1985, A.Ap. Suppl., 60, 285.

Feigelson, E.D., and Nelson, P.I. 1985, Ap.J., 293, 192.

Feldman, F.R., Weedman, D.W., Balzano, V.A., and Ramsey, L.W. 1982, Ap.J., 256, 427.

Filten, J.E. 1976, Ap.J., 207, 700.

Ferland, H., and Netzer, H. 1983, Ap.J., 264, 125.

Ferland, G., and Truran, J.W. 1980, Ap.J., 244, 1022.

French, H.B. 1980, Ap.J. 240, 41.

Frogel, J.A., Persson, S.E., Aaronson, M., and Matthews, K. 1978, Ap.J., 223, 824.

Gehrz, R.D., Sramek, R.A., and Weedman, D.W. 1983, Ap.J., 267, 551.

Geller, M.J., and Huchra, J.P. 1983, Ap.J. Suppl., 52, 61.

Gillett, F.C., Kleinmann, D.e., Whright, E.L., and Capps,R.W. 1975, Ap.J. (Letters), 198, L65.

Giuricin, G., Mardirossian, F., Mezzetti, M., Pisani, A., and Remella, M. 1986, A.Ap., 157, 129.

Glass, I.S. 1973, M.N.R.A.S., 164, 155.

Goldreich, P., and Lynden-Bell, D. 1965, M.N.R.A.S., 130, 125.

Heckmann, T.M. 1980, A.Ap., 87, 152.

Heckmann, T.M. 1983, Ap.J. 268, 628.

Huchra,J.P. 1977a, Ap.J. Suppl., 35, 171.

Huchra,J.P. 1977b, Ap.J. 217, 928.

Huchra, J., Davis, M., Latham, D.,and Tonry, J. 1983, Ap.J Suppl., 52, 89.

References

Huchra, J.P., and Sargent, W.L.W. 1973, Ap.J., 186, 443.

Huchtmeier, W.K., and Richter, O.-G. 1986, A.Ap. Suppl., 64, 111.

Hummel, E. 1981, A.Ap., 96, 111.

"IRAS Catalogues and Atlas Explanatory Supplement", 1985, eds. C.A. Beichman, G. Neugebaur, H.J. Habing, P.E. Clegg, and T.J. Chester (Washington: U.S. Goverment Printing Office).

Jones, B., And Rodrigues-Espinosa, J.M. 1984, Ap.J., 285, 580.

Joseph, R.D., Meikle, W.P.S., Robertson, N.A., and Wright, G.S. 1984, M.N.R.A.S., 157, 309.

Jura, M. 1982, Ap.J., 254, 70.

Karachentsev, D. 1981, Soviet Astronomy Letters, 7, 1.

Keel, W.C. 1980, A.J., 85, 198.

Keel, W.C., Kennicutt, R.C.Jr., Hummel, E., and Van der Hulst, J.M. 1985, A.J., 90, 708.

Kennicutt, R.C.Jr., and Keel, W.C. Ap.J. (Letters), 279, L5.

Kojoian, G., Tovmassian, H.M., Deckinson, D.F., and Dinger, A.S.C. 1980, A.J., 85, 1462.

Larson, R.B., and Tinsley, B.M. 1978, Ap.J., 219, 46.

Lawrence, A., Ward, M., Elvis, M., Fabbiano, G., Willner, S.P., Carleton, N.P., and Longmore, A., 1985, Ap.J., 291, 117.

Lucy, L.B. 1974, A.J., 79, 745.

Lonsdale, C.J., Persson, S.E., and Matthews, K. 1984, Ap.J., 287, 95.

Markarian, B.E. 1967, Astrofizika, 3, 55.

Markarian, B.E. 1969, Astrofizika, 5, 443; 581.

Markarian, B.E. 1972, Astrofizika, 8, 165.

Markaryan, B.E., Erastova, L.K., Lipovetskii, V.A., Stepanyan, Dzh.A., and Shapovalova, A.I. 1985, Astrofizica, 22, 215.

References

Markarian, B.E., Lipovetskii, V.A. 1971, Astrofizika, 7, 511.

Markarian, B.E., Lipovetskii, V.A. 1972, Astrofizika, 8, 155.

Markarian, B.E., Lipovetskii, V.A. 1973, Astrofizika, 9, 487.

Markarian, B.E., Lipovetskii, V.A. 1974, Astrofizika, 10, 307.

Markarian, B.E., Lipovetskii, V.A. 1976, Astrofizika, 12, 389; 687.

Markarian, B.E., Lipovetskii, V.A., and Stepanyan, Dzh. A. 1977, Astrofizika, 13, 225; 397.

Markarian, B.E., Lipovetskii, V.A., and Stepanyan, Dzh. A. 1979, Astrofizika, 15, 363; 549.

Markarian, B.E., Lipovetskii, V.A., and Stepanyan, Dzh. A. 1981, Astrofizika, 17, 619.

Markaryan, B.E., Lipovetskii, V.A., and Stepanyan, Dzh.A. 1983, Astrofizica, 19, 221;

Markaryan, B.E., Lipovetskii, V.A., and Stepanyan, Dzh.A. 1984, Astrofizica, 20, 419.

Markarian, B.E., Oganesyan, E.Y., and Arakelyan, S.N. 1965, Astrofizika, 1, 38.

Markarian, B.E., Oganesyan, E.Y., and Arakelyan, S.N. 1966, Astrofizika, 2, 53.

Moorwood, A.F.M., Glass, I.S. 1982, A.Ap., 115, 84.

Morgan, W.W., and Mayall, N.U. 1957, Pub. A.S.P., 69, 291.

Neyman, J., and Scott, E.J. 1961, Proc. 4th Berkeley Symp. Meth. Stat. and Prob., 3, 261.

Palumbo, G.G.C., Tanzella-Nitti, G., and Vettolani, G. 1983, "CATALOGUE OF RADIAL VELOCITIES OF GALAXIES" (Gordon and Breach Science Publishers).

Rees, M.J. 1984, Ann. Rev. Astr. Ap., 22, 471.

Rieke, G.H. 1978, Ap.J., 226, 550.

Rieke, G.H., and Lebofsky, M.J. 1979, Ann. Rev. Astr. Ap., 17, 477.

References

Rieke, G.H., and Lebofsky, M.J. 1986, Ap.J., 304, 326.

Rieke, G.H., and Lebofsky, M.J. 1980, "Objects of High Redshift", Proc. IAU Symp. No.92, eds Abell, G.O. and Peebles, P.J.E..

Rieke, G.H., and Lebofsky, M.J., Thompson, R.I., Low, F.J., and Tukunaga, A.T. 1980, Ap.J., 238, 24.

Rieke, G.H., and Low, F.J. 1972, Ap.J. (Letters), 176, L95.

Rieke, G.H., and Low, F.J. 1975, Ap.J., 197, 17.

Roche, P.F., Aitken, D.K. 1985, M.N.R.A.S., 213, 789.

Russell, R.W., Soifer, B.T., Merrill, K.M. 1977, Ap.J., 213, 66.

Sandage, A., and Tammann, G.A. 1981, "A Revised Shapley-Ames Catalog of Bright Galaxies" (Washington: Carnegie Institution).

Sargent, W.L.W 1970, Ap.J., 159, 765.

Sargent, W.L.W., and Searle, L. 1970, Ap.J. (Letters), 162, L115.

Schmidt, M. 1968, Ap.J., 151, 353.

Schmitt, J.H.M.M. 1985, Ap.J., 293, 171.

Searle, l., and Sargent, W.L.W. 1972, Ap.J., 173, 25.

Searle, L., Sargent, W.L.W., and Banguolo, W.G. 1973, Ap.J., 179, 427.

Smith, M.G. 1985, "Active Galactic Nuclei", ed. Dyson, J.E., p103.

Soifer, B.T., Rowan-Robinson, M., Houck, J.R., de Jong, T., Neugebauer, G., Aumann, H.H., Beichman, C.A., Boggess, N., Clegg, P.E., Emerson, J.P., Gillett, F.C., Habing, H.J., Hauser, M.G., Low, F.J., Miley, G., and Young, E. 1984, Ap.J. (Letters), 278, L71.

Soifer, B.T., Sanders, D.B., Neugebaers, G., Danielson, G.E., Lonsdale, C.J., Madore, B.F., and Persson, S.E. 1986, Ap.J. (Letters), 304, L41.

References

Sramek, R.A., and Tovmassian, H.M. 1975, Ap.J., 196, 339.

Sramek, R.A., and Weedman, D.W. 1986, Ap.J., 302, 604.

Stocke, J.T. 1978, A.J., 83, 348.

Sulentic, J.W. 1976, A.J., 81, 582.

Terlevich, R., and Melnick, J. 1985, M.N.R.A.S., 213, 841.

Thuan, T.X. 1983, Ap.J., 268, 667.

Toomre, A., and Toomre, J. 1972, Ap.J., 178, 623.

Tully, R.B., and Fisher, J.R. 1977, A.Ap., 54, 661.

Turner, E.L., and Gottii, J.R. 1976, Ap.J. Suppl., 32, 409.

Turner, E.L. 1979, Ap.J., 231, 645.

Van den Bergh, S. 1975, Ann. Rev. Astr. Ap., 13, 217.

Van den Heuvel, E.P.J. 1980, "X-ray Astronomy", Proc. NATO Advanced Study Institute, Erice, Sicily, July 1-14, 1979; eds Giancconi, R. and Setti, G. (Dordrecht: Reidel), p119.

Veron-Cetti, M.P., and Veron, P. 1984, Eso Sci. Report No.1.

Weedman, D.W. 1970, Ap.J., 159, 405.

Weedman, D.W. 1973, Ap.J., 183, 29.

Weedman, D.W. 1985, Bull. A.A.S., 17, 846.

Whitemore, B.C., and Kirshner, R.P. 1981, Ap.J., 250, 43.

Whitemore, B.C., Kirshner, R.P., and Schechter, P.L. 1979, Ap.J., 234, 68.

Willner, S., Soifer, B.T., Russell, R.W., Joyce, R.R., and Gillett, F.C. 1977, Ap.J. (Letters), 217, L121.

Windhorst, R.A., Miley, G.K., Owen, R.N., Kron, R.G., and Koo, D.C. 1985, Ap.J., 289, 494.

Wright, A.E. 1972, M.N.R.A.S., 157, 309.

Zwicky, F., Herzog, E., Wild, P., Karpowicz, M., and Kowal, C. 1961-1968, "Catalogue of Galaxies and Clusters of Galaxies"

References

(Pasadena: California Institute of Technology).

FIGURES

Fig. 2.1 Morphological distributions of galaxies with starburst nuclei compared with Markarian galaxies and field galaxies. (From Balzano (1983).)

Fig. 3.1.1 Color-color diagram of Markarian galaxies. (From Weedman (1973).)

Fig. 3.1.2 Color-color diagram of Markarian galaxies. (From Huchra (1976a).)

Fig. 3.1.3 Color-color diagram predictcted by composite models with different contributions of burst. (From Huchra (1976b).)

Curve 1: a1=1.35, a0=2.35, t0=1.5*10**9 yrs.

Curve 2: a1=1.35, a0=2.35, t0=5*10**9 yrs.

Curve 3: a1=2.35, a0=2.35, t0=1.5*10**9 yrs.

Fig. 3.1.4 Color-color evolution of two composite models. (From Huchra (1976b).)

Curve 1: a1=1.35, a0=2.35, t0=1.5*10**9 yrs. (Evolutionary locus of a model corresponding to the square in Fig. 3.1.3.)

Curve 2: a1=1.35, a0=2.35, t0=5*10**9 yrs. (Evolutionary locus of a model corresponding to the triangle in Fig. 3.1.3.)

Fig. 3.1.5 Color-color diagram of peculiar galaxies. (From Larson and Tinsley (1978).)

Fig. 3.2.1 Line ratios diagram of starburst galaxies. (From Balzano (1983).)

Fig. 3.3.1 U-B vs J-K diagram of starburst galaxies compared with Seyferts. (From Balzano and Weedman (1981).)

Fig. 3.3.2 Distribution of infrared colors of starburst nuclei compared with bright NGC nuclei. (From Balzano (1983).)

Fig. 3.3.3 J-H vs H-K diagram of compact dwarf galaxies. (From Thuan (1983).)

Fig. 3.4.1 IR to blue luminosity ratio vs far-IR monochromatic flux density ratios of Revised Shapley-Ames galaxies. (From De

Figures

Jong et al (1984).)

Fig 3.4.2 Flux density distributions of starburst nuclei. (From Lawrence et al (1984).)

Fig. 4.1.1 Optical luminosity function of Markarian galaxies. (From Huchra (1977a).)

Fig. 4.2.1 Surface density analysis.

Fig. 4.2.2 Surface density distribution (uncorrected). Fractional friquency (percentage) vs density (/(80 sq deg)).

Fig. 4.2.3 Surface density distribution (corrected). Fractional friquency (percentage) vs density (/(80 sq deg)).

Fig. 4.2.4a Blue luminosity function of Markarian galaxies (total) compared with Huchra's (1977a).

Fig. 4.2.4b Blue luminosity function of Markarian galaxies (stellar).

Fig. 4.2.4c Blue luminosity function of Markarian galaxies (diffuse).

Fig. 4.2.8 Correlation between monochromatic luminosities at 60 microns and at 4400 A (erg/sec/Hz).

Fig. 4.2.9 Correlation between IR and blue luminosities.

Fig. 4.2.8 Monochromatic luminosity function (60 microns) of Markarian galaxies.

Fig. 4.2.9 Integrated IR luminosity function of Markarian galaxies.

Fig. 5.1 Color-color diagrams of a. noninteracting peculiar galaxies, b. interacting peculiar galaxies. (From Larson and Tinsley (1978).)

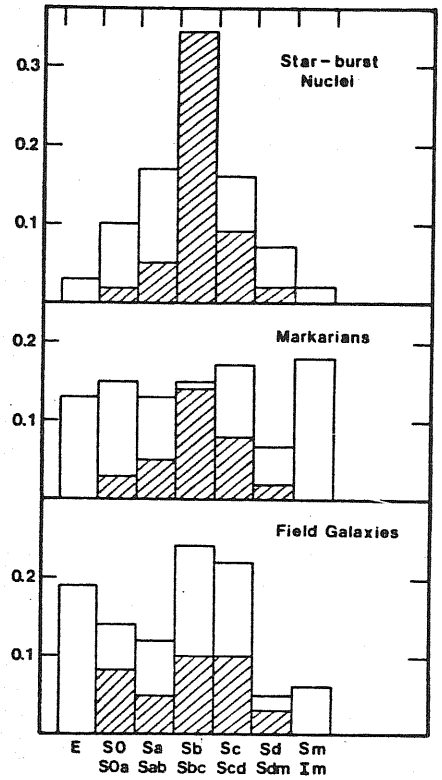

FIG. 2.—Morphology distributions. The sample sizes have been normalized to unity. The shaded areas denote the percentage of barred spirals.

Fig.2.1

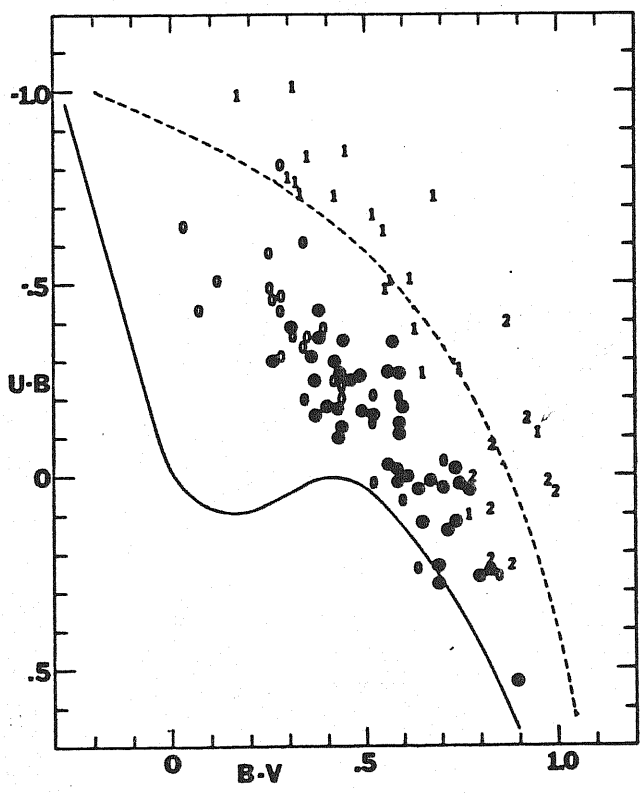

FIG. 1.—Color-color diagram for galaxies in table 1; observed colors listed in the table plotted after correcting for galactic reddening. *Filled circles*, BN (bright nucleus) galaxies; *open circles*, D (diffuse) galaxies; *numbers "1,"* Seyfert galaxies of type 1; *numbers "2,"* Seyfert galaxies of type 2. *Dashed curve*, Sandage's locus of the color changes expected as a galaxy like M31 (*lower right*) is increasingly dominated by the superposed light from a typical QSO.

Fig. 3.1.1

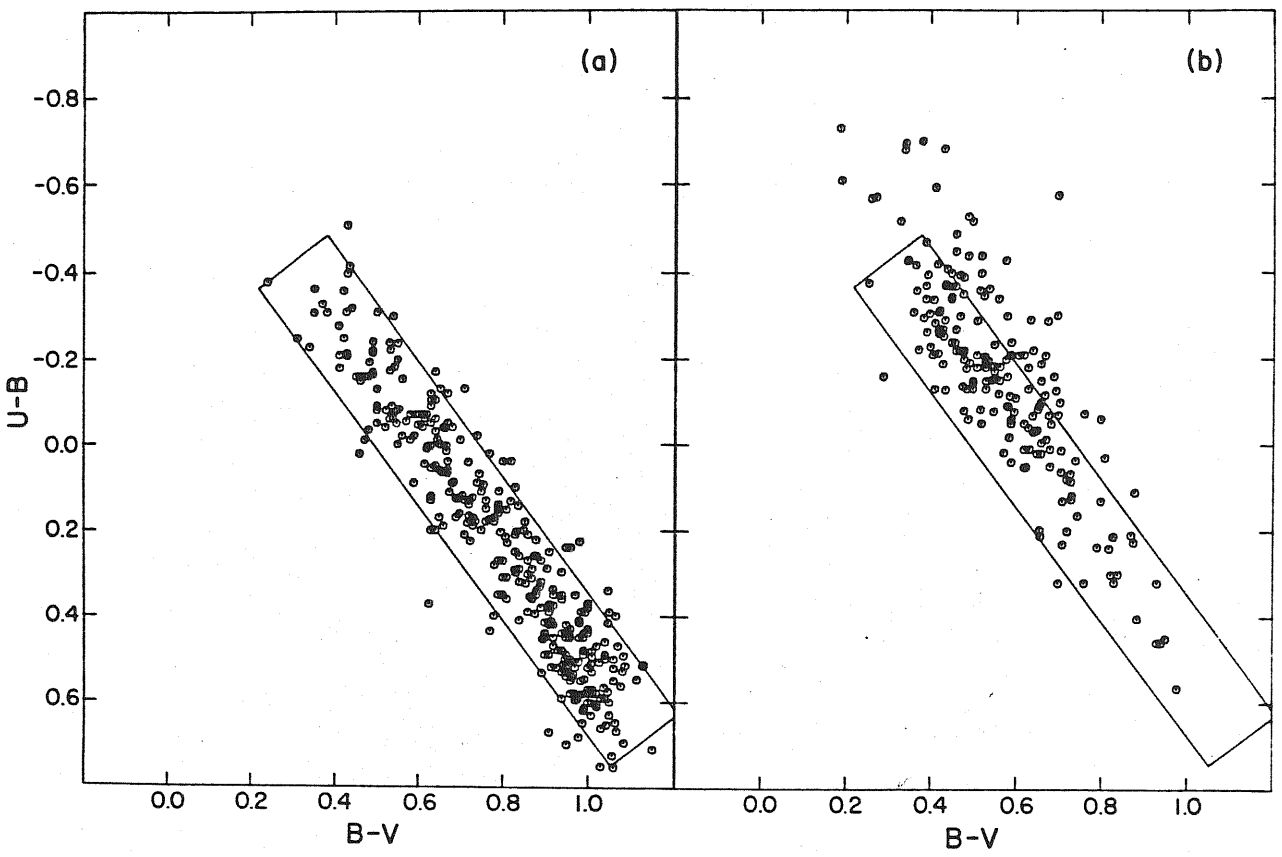

FIG. 2.—(*a*) The color-color distribution of field galaxies. The rectangular envelope is described in the text. (*b*) The color-color distribution of Markarian galaxies superposed on the field-galaxy envelope.

Fig. 3.1.2

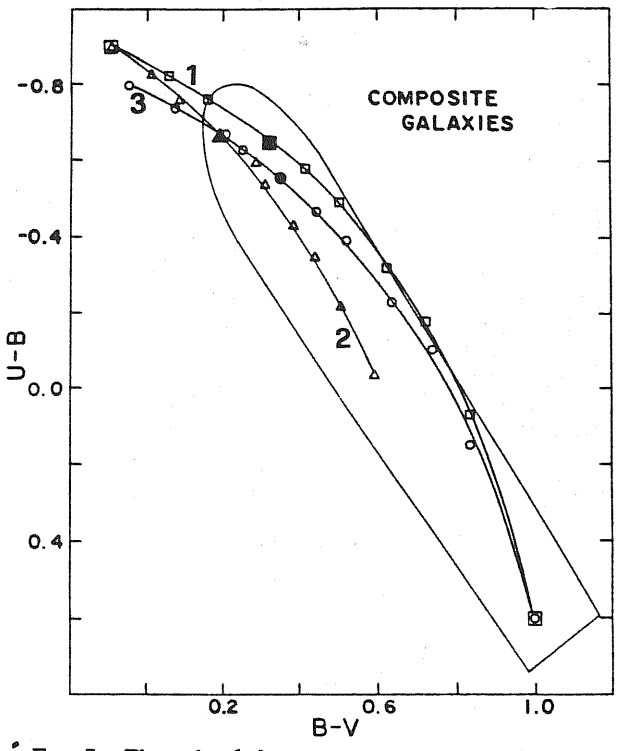

FIG. 7.—The colors of two-component composite galaxy models. The points along the curves represent different contributions of the burst to the model's total *V*-band light, ranging from zero at the lowest points on the curves to 100% at the uppermost points. The filled square, triangle, and circle represent models where the burst contributes 50% of the light.

Fig. 3.1.3

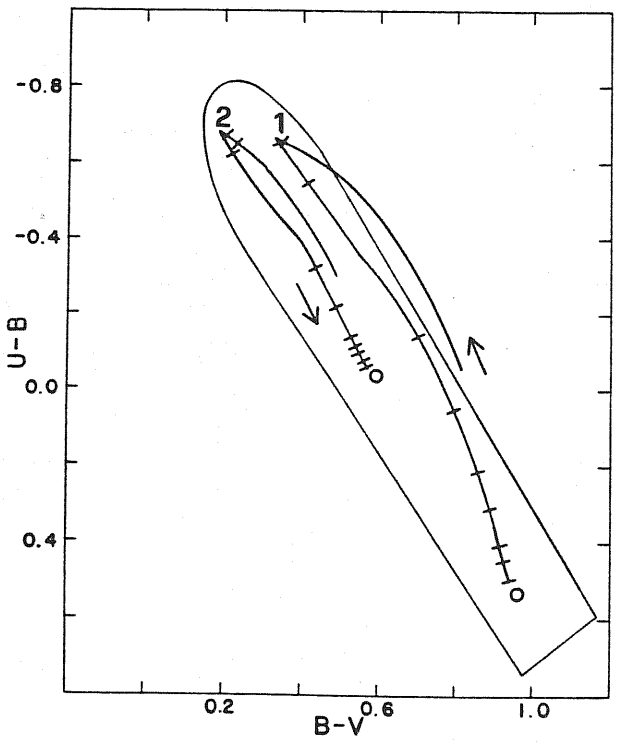

FIG. 8.—The color evolution of two composite galaxy models. The burst is the same for both, $\alpha = 1.35$ and duration 2.5×10^7 years, but different underlying galaxy models (*circles*) have been added. The ticks along the tracks represent steps of 10^7 years, and a total time of 10^8 years is shown.

Fig. 3.1.4

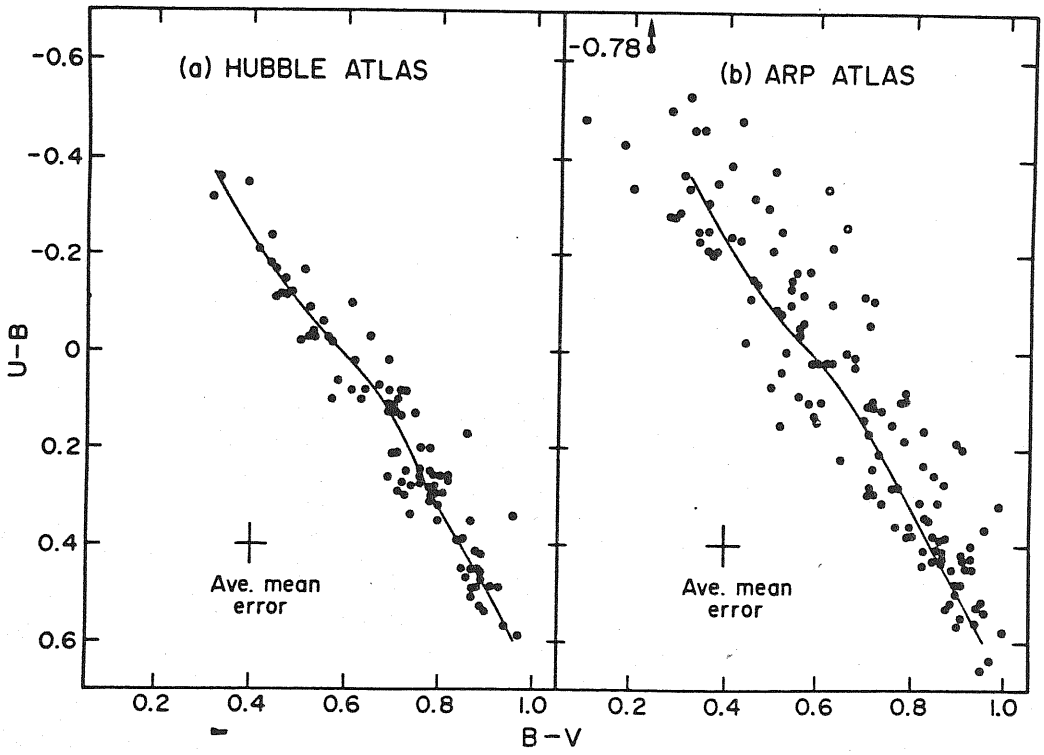

FIG. 1.—The two-color plots for morphologically normal and peculiar galaxies with latitudes $|b| > 20°$. Panel (*a*) shows all Hubble Atlas galaxies with colors in the RC2 that are not in sample (*b*). Panel (*b*) shows Arp Atlas galaxies with colors in the RC2, plus a few with colors from other sources listed in the text; the two open circles are Type I Seyfert galaxies. The curve in both plots is an eye-estimated mean line through the Hubble Atlas sample. The average mean errors of the RC2 colors for each sample are indicated.

Fig. 3.1.5

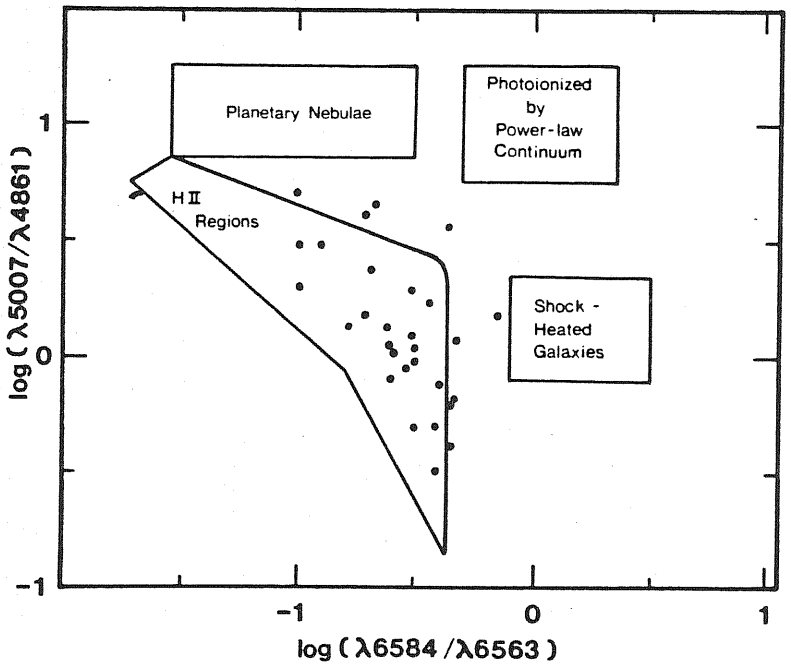

FIG. 3.—Line ratio correlations. Diagram is taken from Baldwin, Phillips, and Terlevich 1981. Envelopes indicate typical ranges for the [N II]/Hα and [O III]/Hβ line ratios of four different astrophysical objects. Data points represent star-burst nuclei.

Fig. 3.2.1

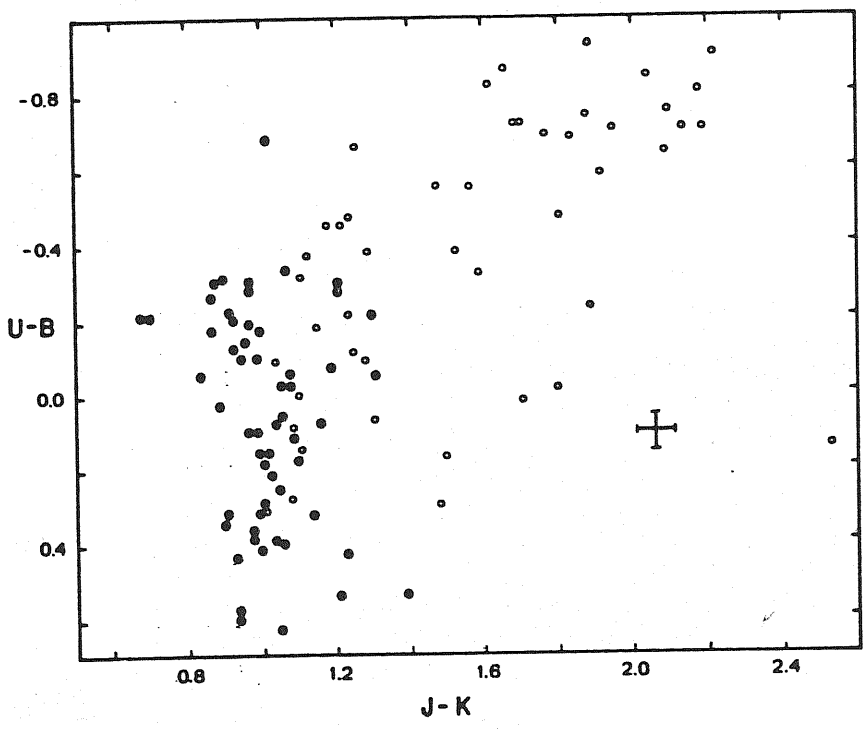

FIG. 4.—Comparison of $(U-B)$ and $(J-K)$ colors for galactic nuclei. *Filled circles:* galaxies not spectroscopically classified as Seyfert galaxies; *open circles:* galaxies spectroscopically classified as Seyfert galaxies. Representative error bars are shown.

Fig. 3.3.1

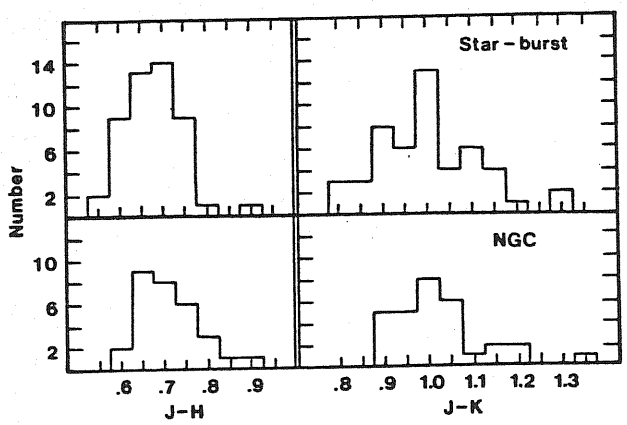

FIG. 6.—Distribution of infrared colors for star-burst nuclei and bright NGC nuclei.

Fig. 3.3.2

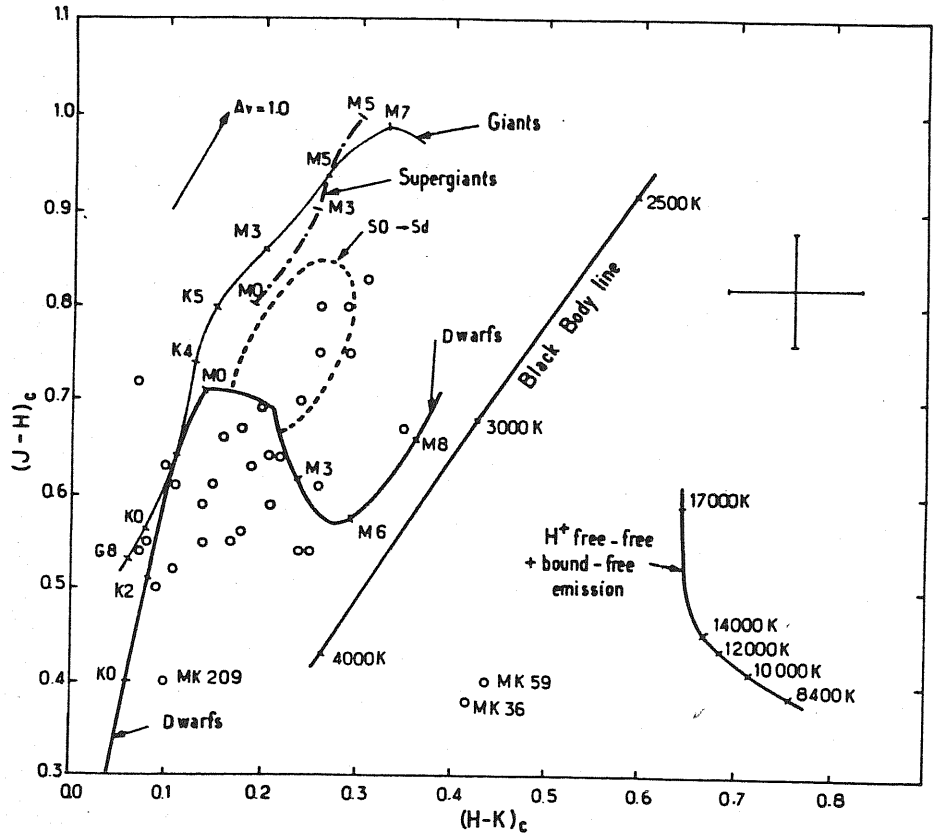

FIG. 1.—The blue compact dwarf galaxies observed are plotted in the JHK plane as open circles. The infrared colors have been corrected for galactic extinction. The free-free and free-bound emission from hydrogen ions and the blackbody line are shown for the range of temperatures of interest. The mean color lines for dwarfs and giants are from Frogel *et al.* (1978), with the $J-H$ colors transformed to the Johnson (1966a) system. The mean color line for M supergiants has been taken from Lee (1970). The extinction arrow corresponds to $A_V = 1$ and van de Hulst curve no. 15 (Johnson 1968). The errors bars represent the mean of the errors in the colors of all galaxies observed. The region within the dashed line represents the location of the galaxies of type S0 to Sd studied by Aaronson (1977). The galaxies Haro 2 $[(J-H)_c = -0.01, (H-K)_c = 0.25]$ and Haro 3 $[(J-H)_c = -0.08, (H-K)_c = 0.17]$ are off-scale and are not plotted.

Fig.3.3.3

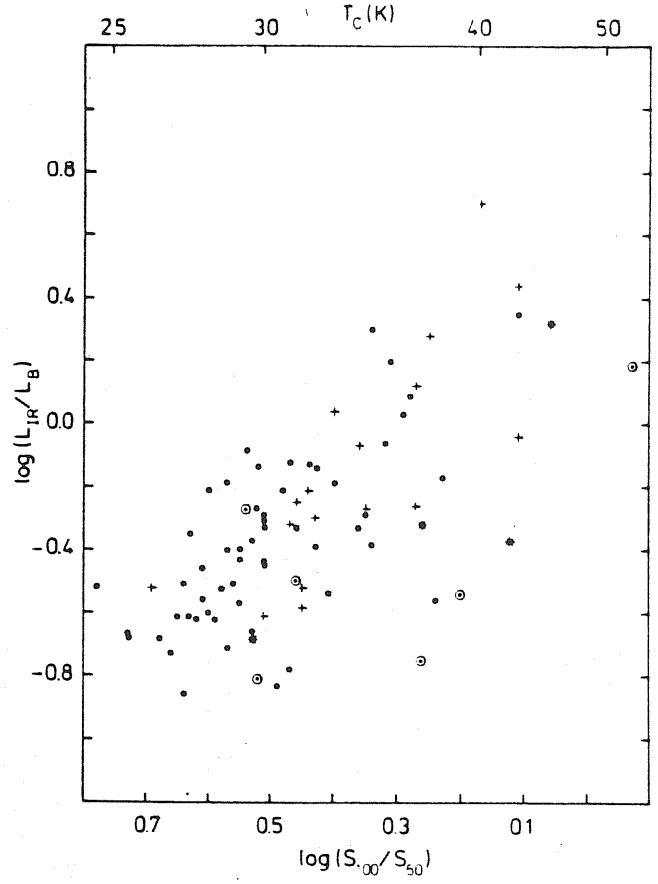

FIG. 2.—Infrared to blue luminosity ratios versus far-infrared monochromatic flux density ratios. The upper scale gives color temperatures for a dust emissivity proportional to frequency. Separate symbols are used to indicate lenticulars (*dotted circles*), normal spirals (*dots*), barred spirals (*pulses*), and irregulars (*stars*).

Fig. 3.4.1

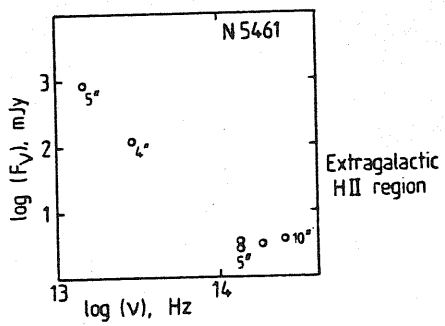

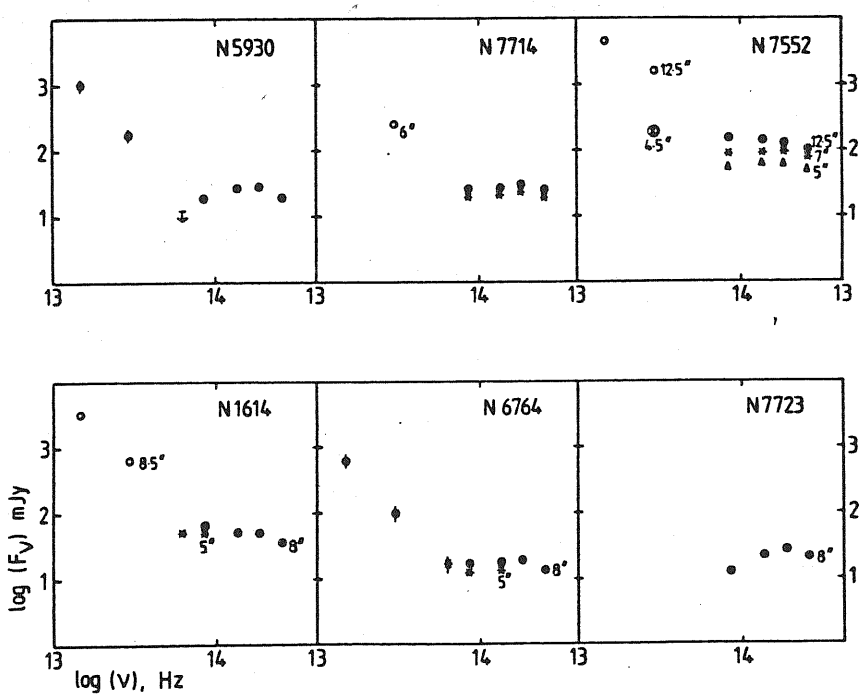

FIG. 1c.—Flux density distributions of starburst nuclei

Fig. 3.4.2

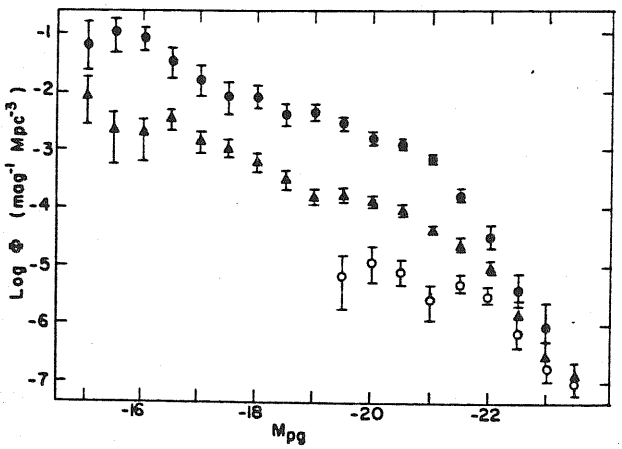

FIG. 4.—Log space density (galaxies per cubic megaparsec per absolute magnitude interval) versus absolute photographic magnitude for field galaxies (*filled circles*), Markarian galaxies (*filled triangles*), and Markarian Seyfert galaxies (*open circles*).

Fig. 4.1.1

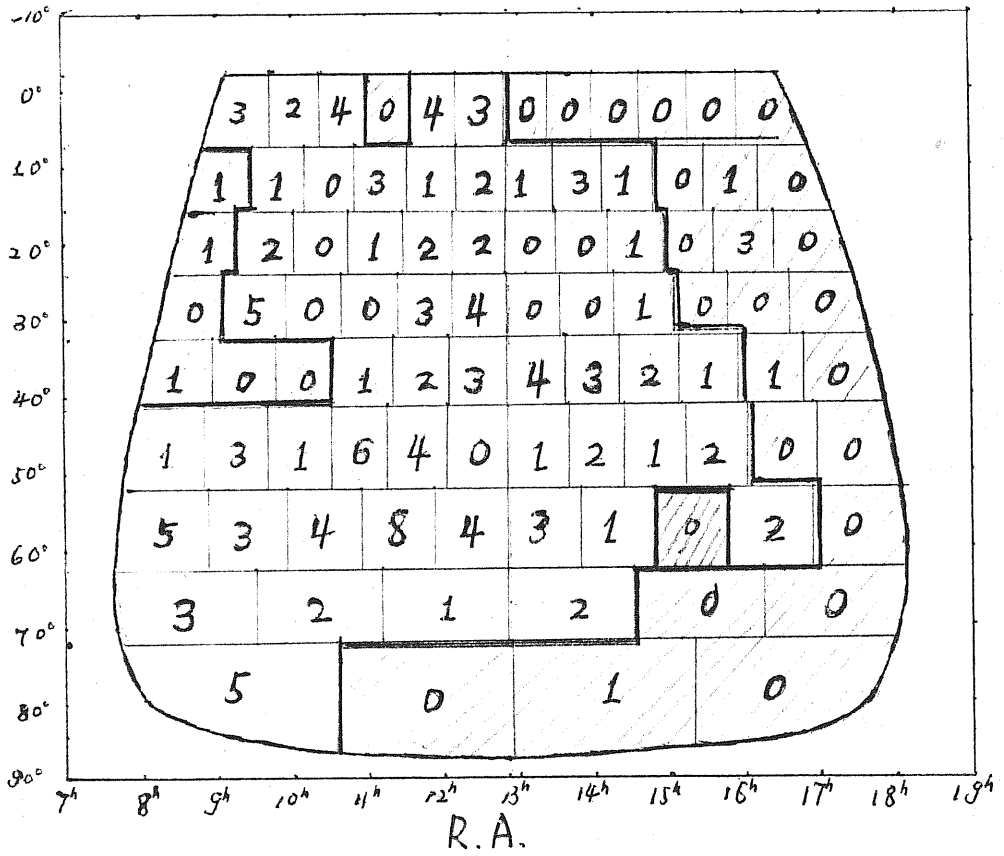

Fig. 4.2.1a

Sky region with boundaries : $b^{II} = 30°$ and $\delta = -2$. Small squars are subregions, the numbers in them is number of galaxies. Regions with dark lines are supposed to be "bad regions" and are excluded from our sample.

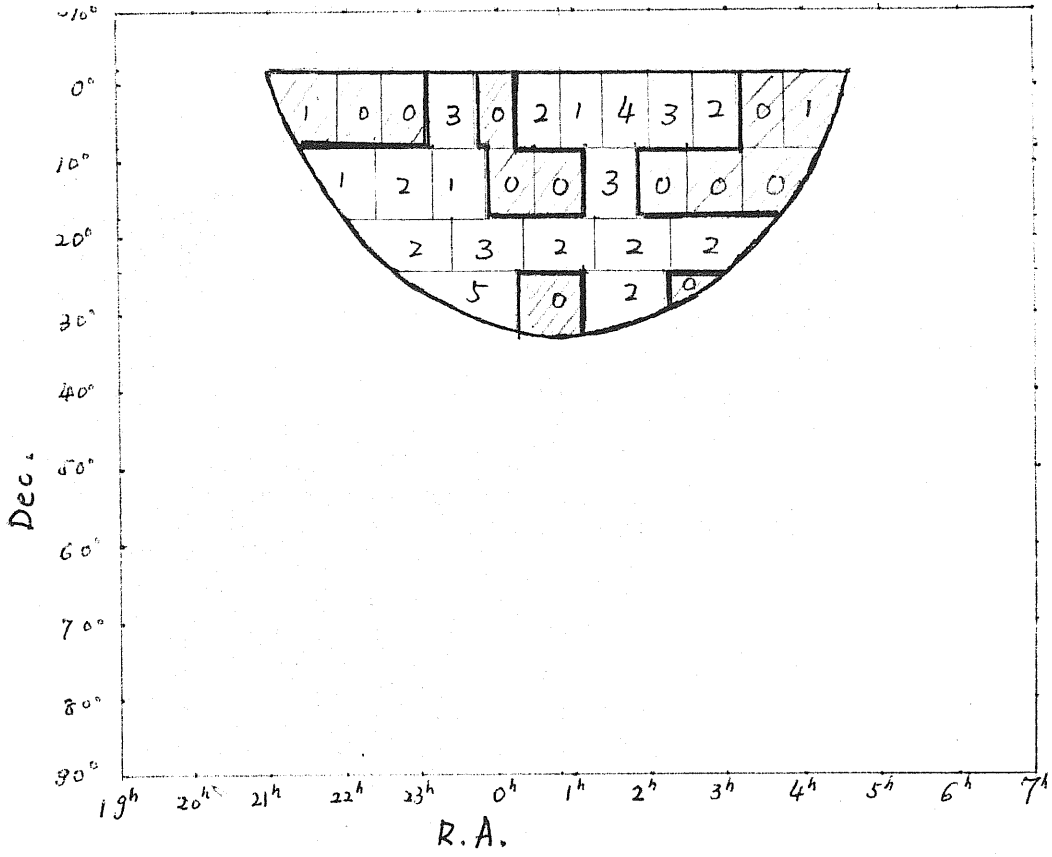

Fig. 4.2.1b

Sky region with boundaries $b^{II} = -30°$ $\delta = -2$.

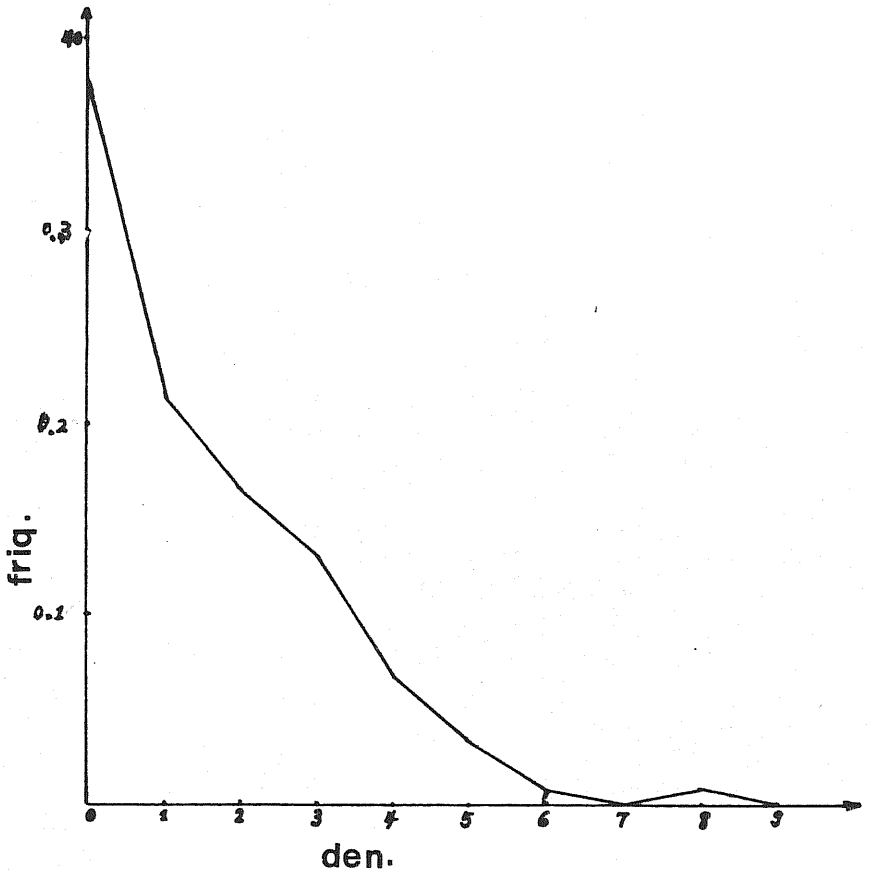

Fig.4.2.2

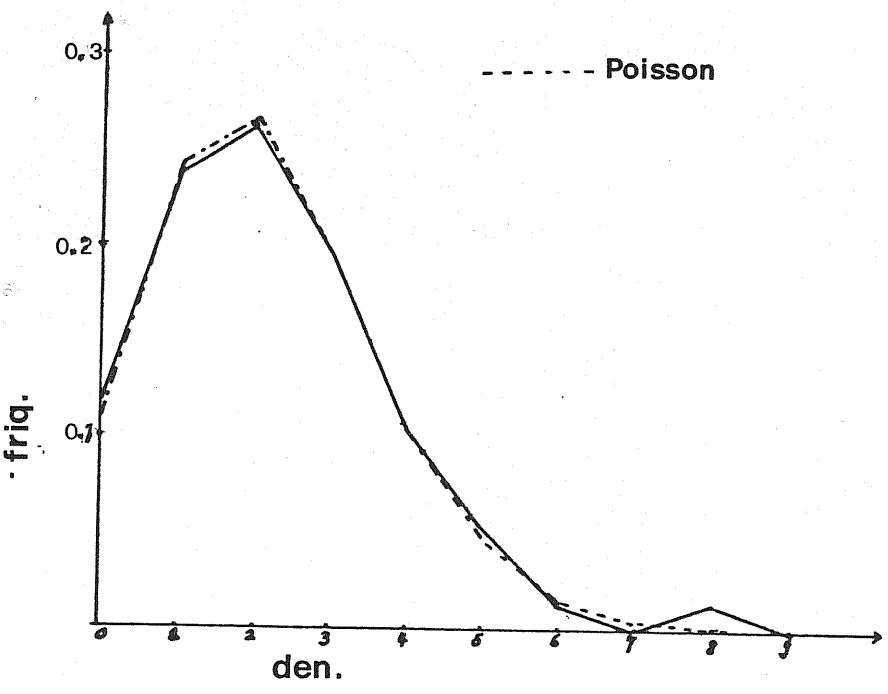

Fig .4.2.3

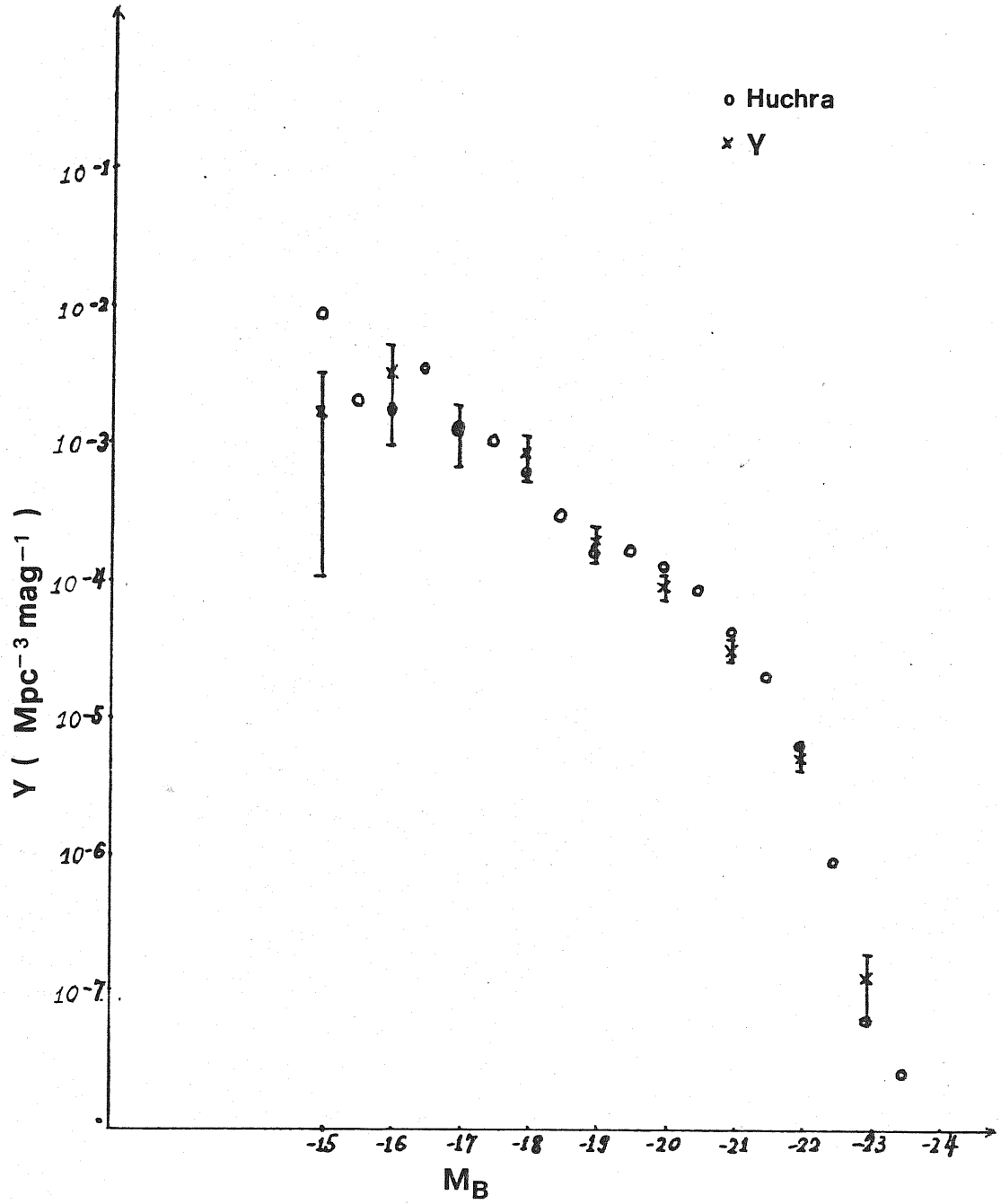
o Huchra
× Y
10 -1
10 -2
10 -3
10 -4
10-5
10-6
10-7
Y (Mpc-3 mag-1)
-15
-16
-17
-18
-19
-20
-21
-22
-23
-24
MB

Fig. 4.2.4a

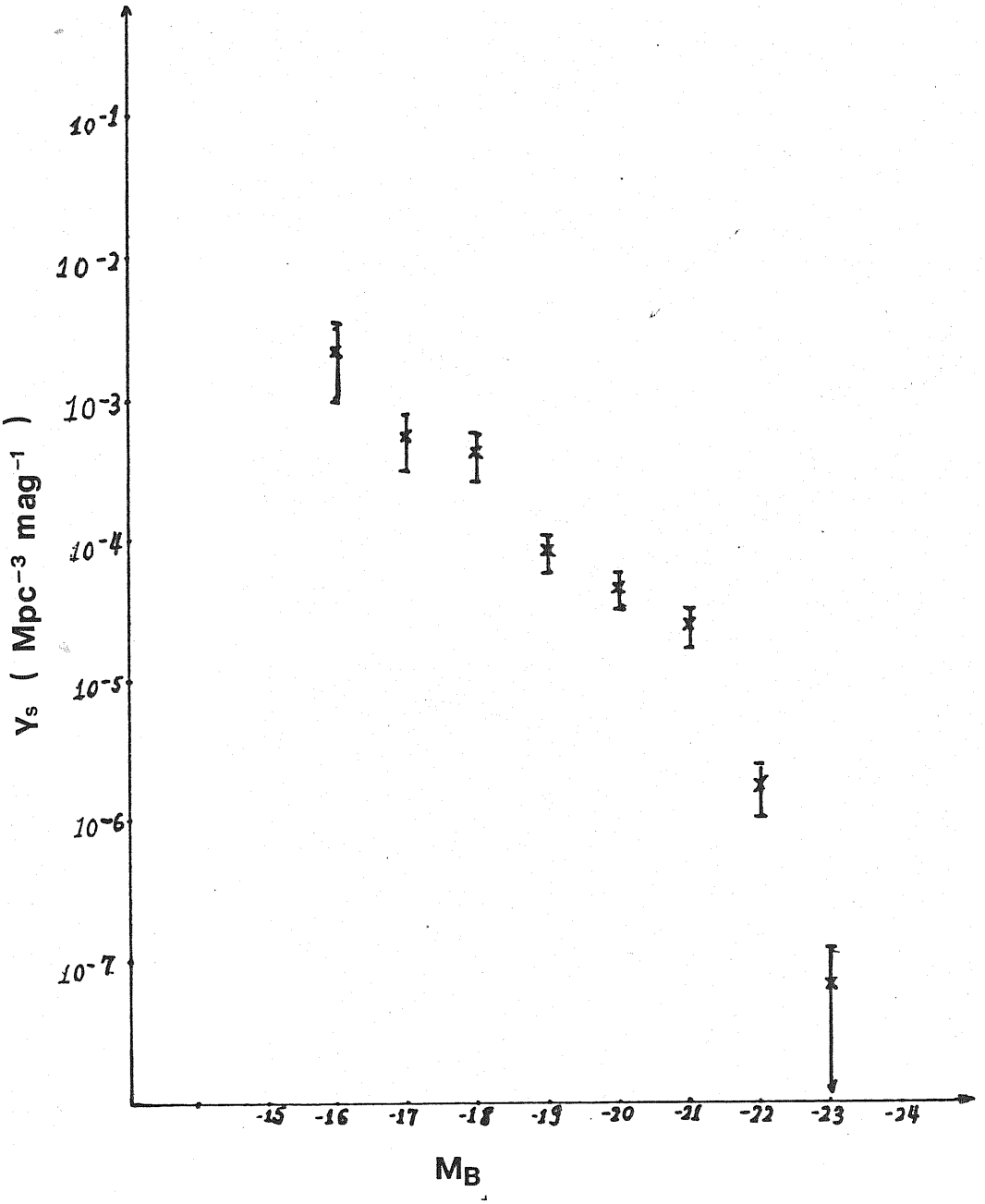
10^{-1}
10^{-2}
10^{-3}
10^{-4}
10^{-5}
10^{-6}
10^{-7}
Y_s (Mpc^{-3} mag^{-1})
-15
-16
-17
-18
-19
-20
-21
-22
-23
-24
M_B

Fig. 4.2.4b

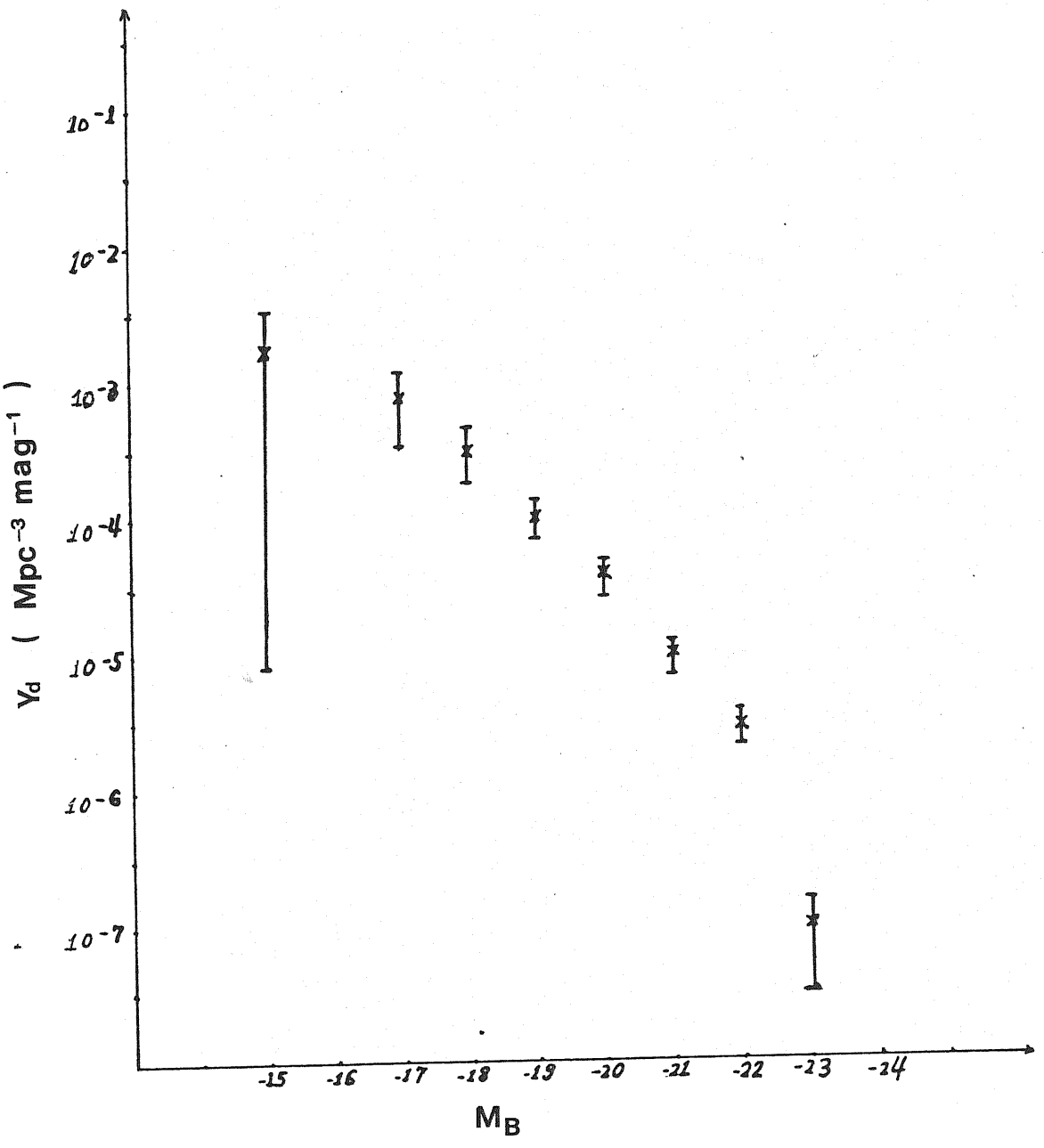
10^{-1}
10^{-2}
10^{-3}
10^{-4}
10^{-5}
10^{-6}
10^{-7}
Y_d (Mpc^{-3} mag^{-1})
-15
-16
-17
-18
-19
-20
-21
-22
-23
-24
M_B

Fig. 4.2.4c

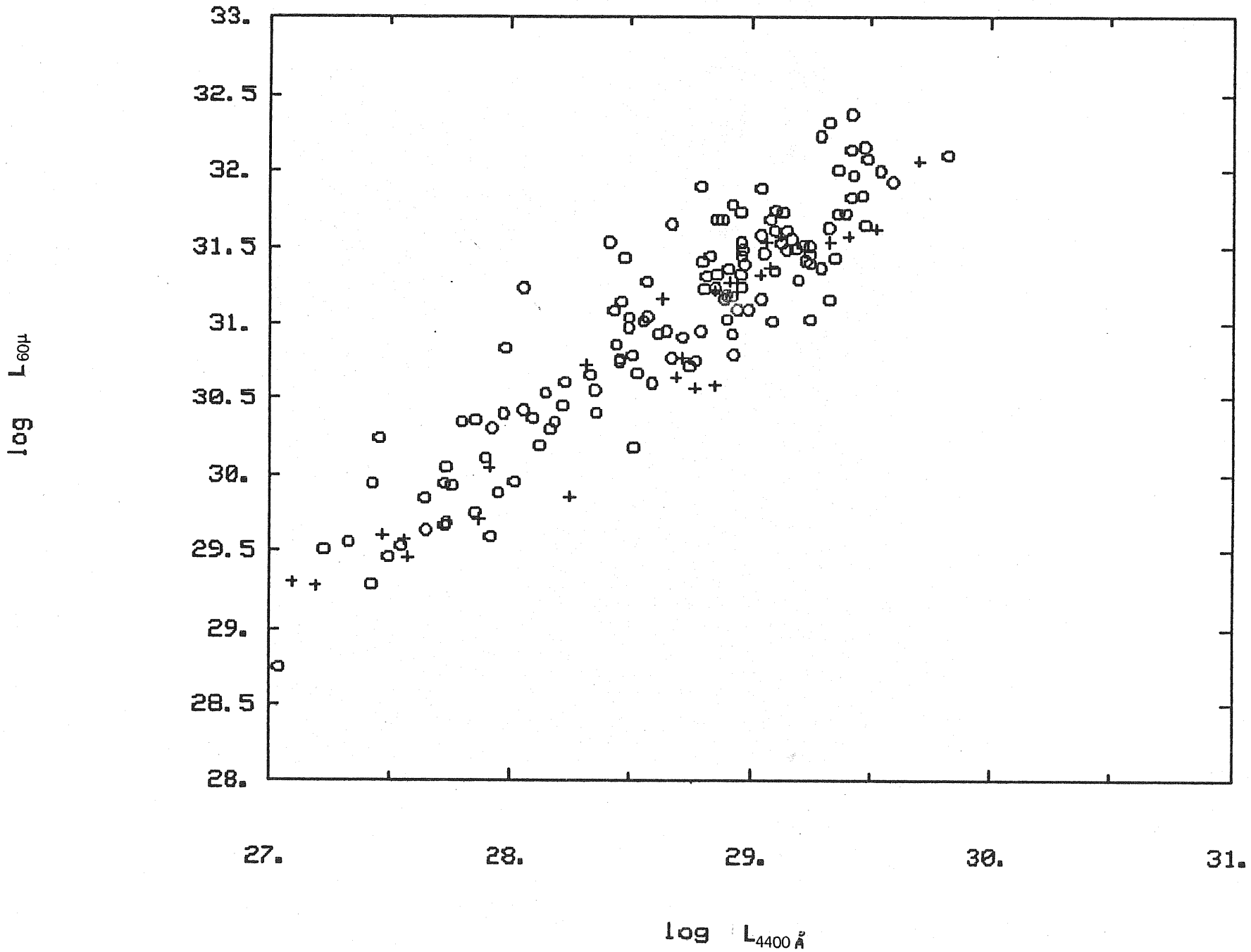
33.
32.5
32.
31.5
31.
30.5
30.
29.5
29.
28.5
28.
27.
28.
29.
30.
31.
log $L_{60\mu}$
log $L_{4400\,\text{Å}}$

Fig. 4.2.8

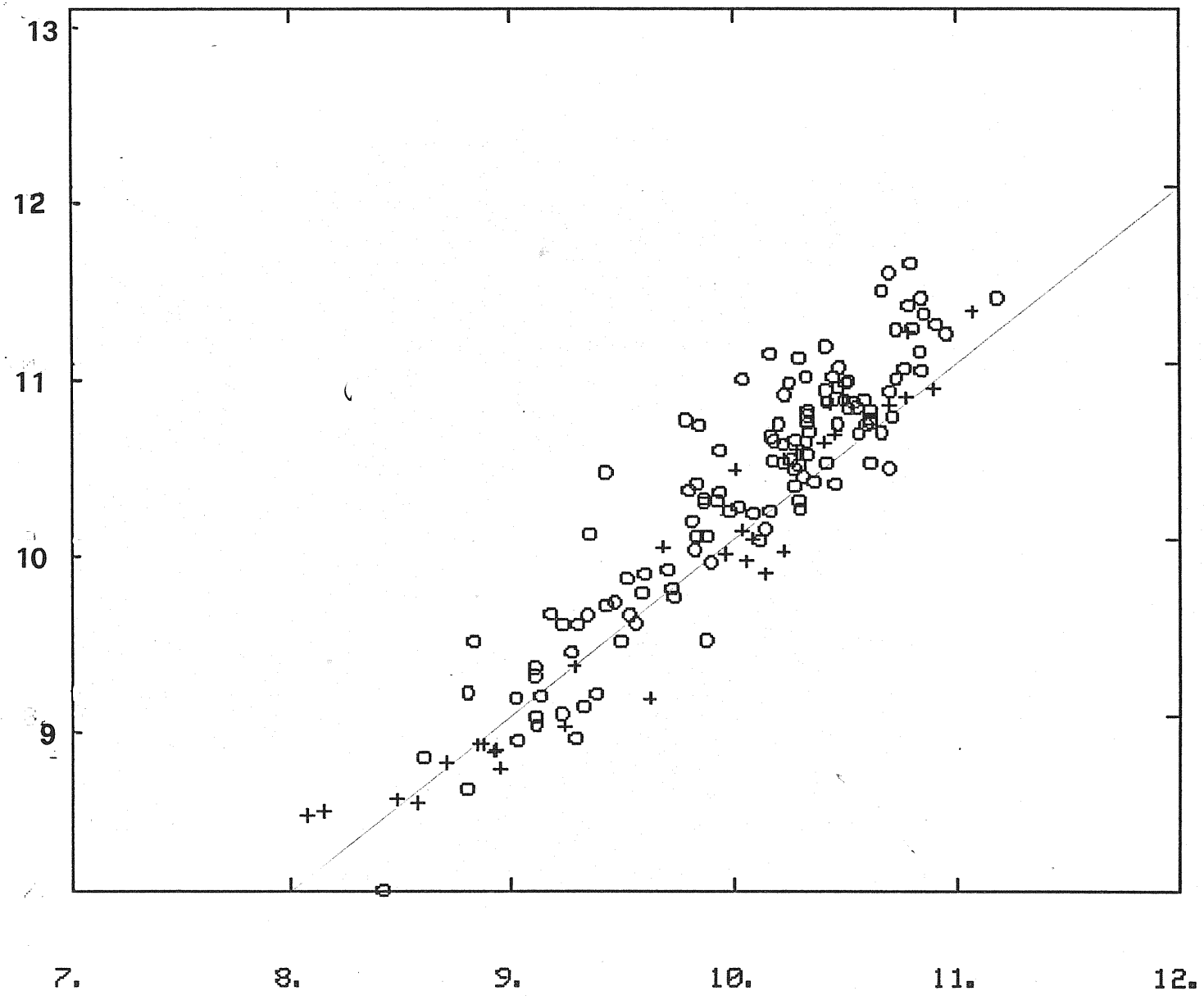

Fig. 4.2.9

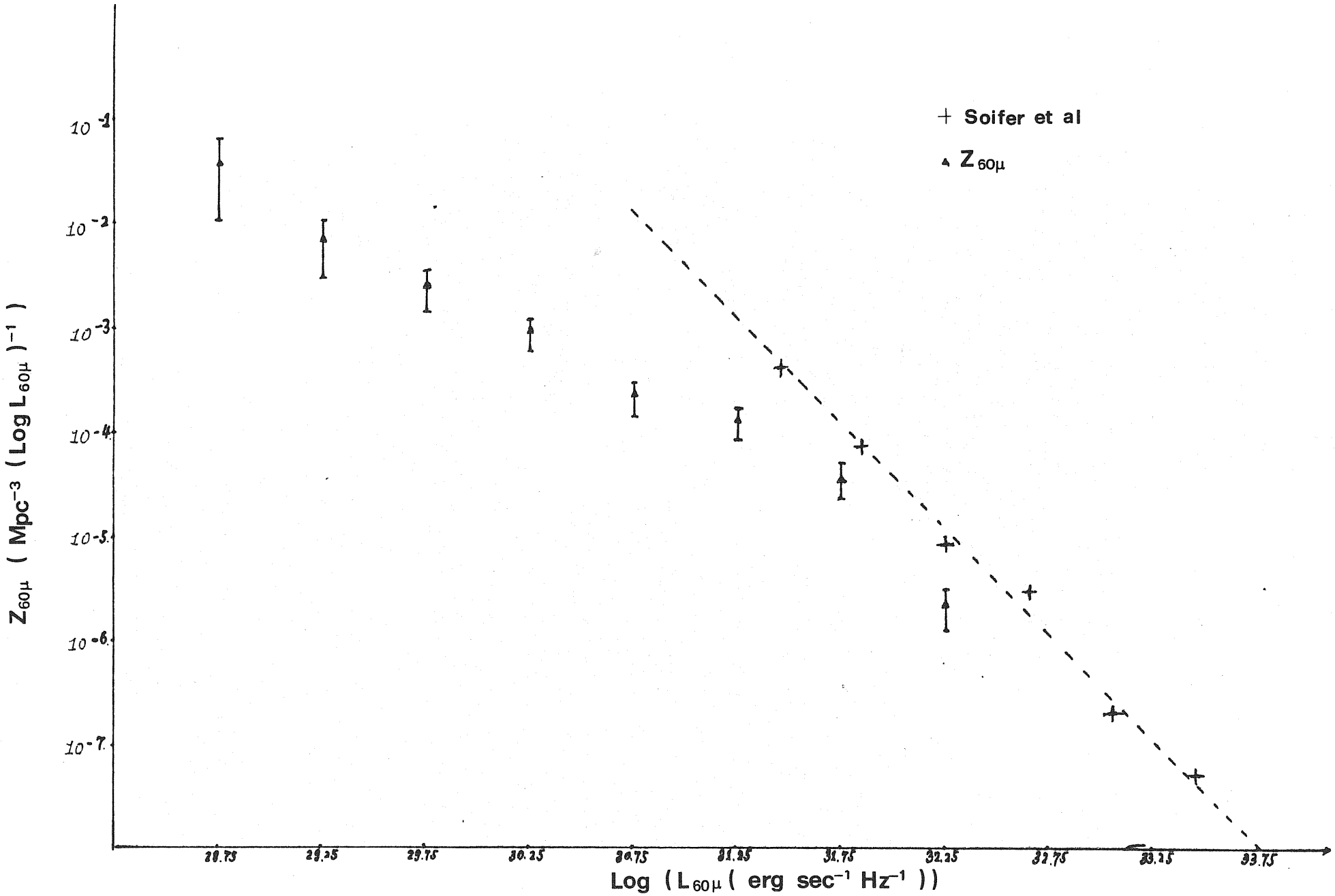
+ Soifer et al
▲ $Z_{60\mu}$
10^{-1}
10^{-2}
10^{-3}
10^{-4}
10^{-5}
10^{-6}
10^{-7}
$Z_{60\mu}$ (Mpc^{-3} (Log $L_{60\mu}$)$^{-1}$)
28.75
29.25
29.75
30.25
30.75
31.25
31.75
32.25
32.75
33.25
33.75
Log ($L_{60\mu}$ (erg sec^{-1} Hz^{-1}))

Fig. 4.2.10

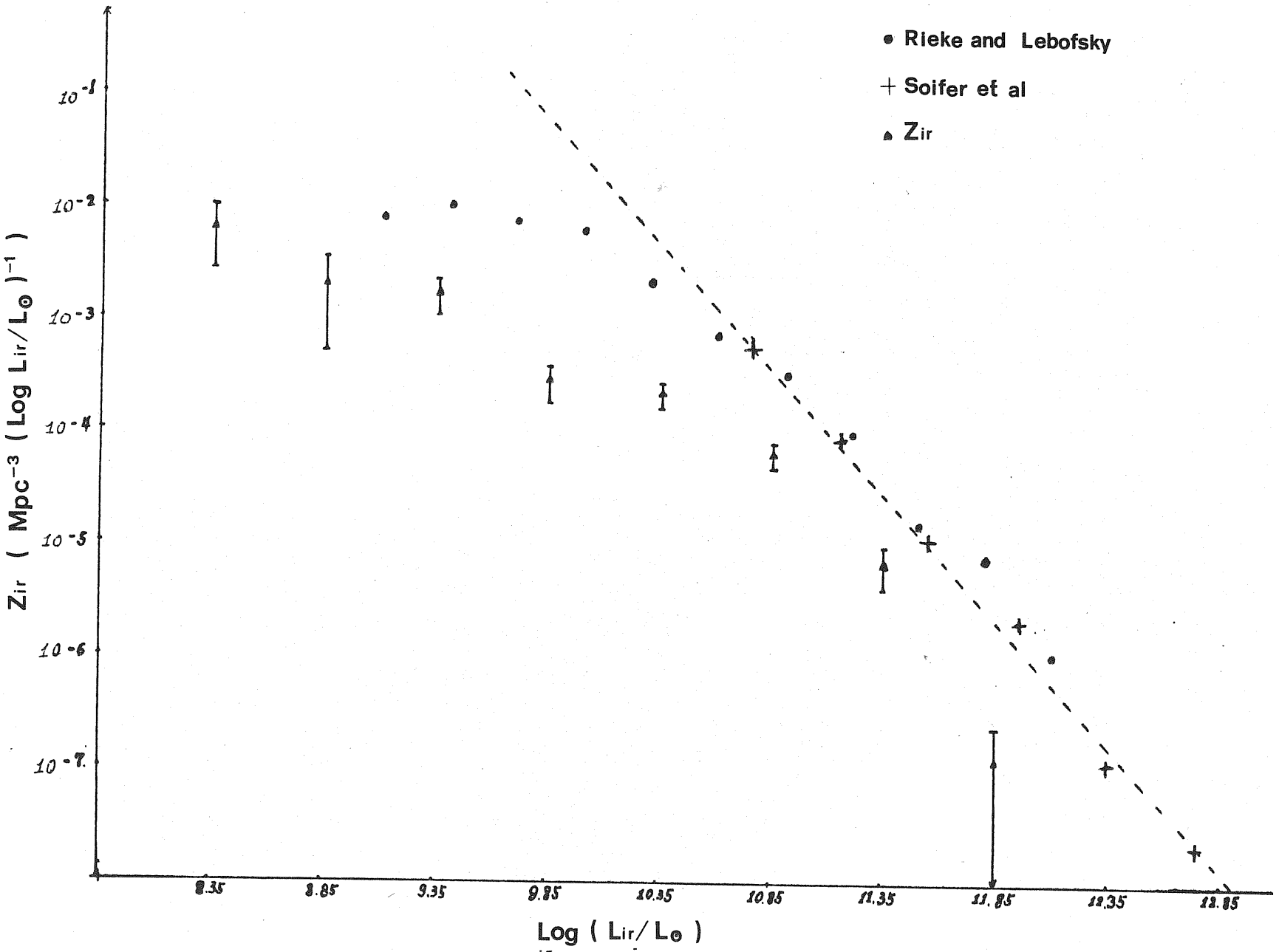
• Rieke and Lebofsky
+ Soifer et al
▲ Zir
10^{-1}
10^{-2}
10^{-3}
10^{-4}
10^{-5}
10^{-6}
10^{-7}
Z_{ir} (Mpc^{-3} (Log $L_{ir}/L_{\odot}$)$^{-1}$)
8.35
8.85
9.35
9.85
10.35
10.85
11.35
11.85
12.35
12.85
Log ($L_{ir}/L_{\odot}$)

Fig. 4.2. 11

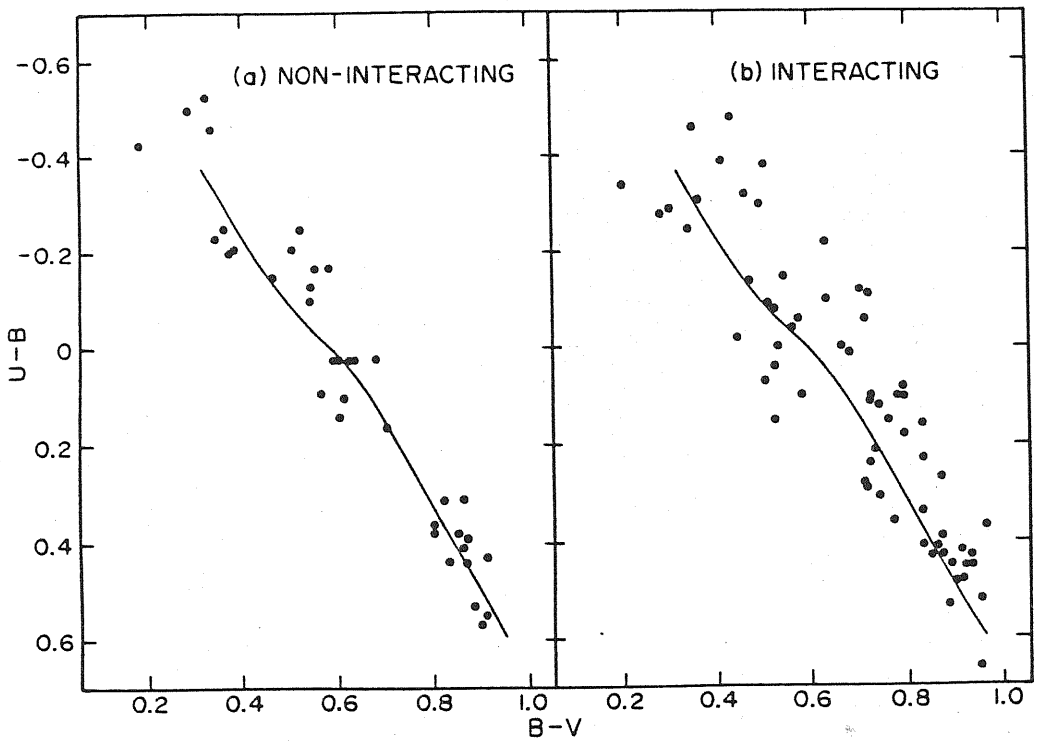

FIG. 4.—The two-color plots of Arp galaxies classified as (*a*) noninteracting or (*b*) interacting. The Arp numbers of the galaxies in each group are given in Table 3. The solid line in each plot is the empirical normal relation for the Hubble galaxies in Fig. 1*a*.

Fig. 5.1

TABLE 3.2.1

EMISSION LINE CORRELATIONS

Y^*	X^*	R	α^*	β^*
log W(Hβ).....	$U-B$	−0.65	0.61 ± 0.05	−1.39 ± 0.16
log W(Hβ).....	M_B	+0.49	0.86 ± 0.04	+0.11 ± 0.02
E.....	M_B	+0.45	1.88 ± 0.15	+0.30 ± 0.07
E.....	$U-B$	−0.44	1.47 ± 0.22	−3.16 ± 0.70
E.....	log W(Hβ)	+0.35	1.08 ± 0.37	+1.14 ± 0.33
USB.....	log W(Hβ)	−0.35	21.53 ± 0.11	−0.40 ± 0.11
log W(Hβ).....	$B-V$	−0.28	1.45 ± 0.17	−0.93 ± 0.31
E.....	$B-V$	−0.24	3.61 ± 0.60	−2.63 ± 1.15
BSB.....	E	+0.18	21.20 ± 0.09	+0.06 ± 0.03

* Fitted to the equation $Y = \alpha + \beta X$.

TABLE 3.3.1

COLOR DISTRIBUTIONS

Type	Star Burst	E and S0	Bright NGC
$J-H$	0.70+0.06	0.71+0.05	0.73+0.07
$J-K$	1.02+0.12	0.95+0.08	1.04+0.10
Sample size ...	50	51	30

TABLE 4.2.1 SURFACE DENSITY DISTRIBUTION (UNCORRECTED)

Surf. den. <1>	Friq. <2>	Fraction (%) <3>
0	45	37.5
1	26	21.3
2	20	16.4
3	16	13.1
4	8	6.6
5	4	3.3
6	1	0.8
7	0	0.0
8	1	0.8
9	0	0.0

TABLE 4.2.2 SURFACE DENSITY DISTRIBUTION (CORRECTED)

Surf. den. <1>	Friq. <2>	Fraction (%) <3>	Poisson <4>
0	9	11.8	11.1
1	18	23.7	24.4
2	20	26.3	26.8
3	15	19.7	19.7
4	8	10.5	10.8
5	4	5.3	4.8
6	1	1.3	1.7
7	0	0.0	0.5
8	1	1.3	0.2
9	0	0.0	>0.1

TABLE 4.2.3 OPTICAL SAMPLE

MK <1>	A <2>	D <3>	Z <4>	R <5>	Mz <6>	EBV <7>
12	7 44 41.0	74 29 6	0.0140	1	12.70	0.03
13	7 51 56.8	60 26 18	0.0050	1	14.50	0.03
14	8 5 21.7	72 56 33	0.0110	1	14.40	0.03
18	8 58 1.6	60 20 53	0.0110	1	14.30	0.03
25	10 0 22.2	59 40 43	0.0090	1	14.20	0.01
33	10 29 22.2	54 39 23	0.0050	1	13.20	0.00
35	10 42 16.4	56 13 20	0.0040	1	12.90	0.00
49	12 16 36.4	4 8 7	0.0050	1	14.50	0.00
52	12 23 8.9	0 51 0	0.0070	1	12.40	0.01
59	12 56 38.2	35 6 50	0.0030	1	12.80	0.00
84	7 51 5.7	55 50 7	0.0200	1	13.60	0.03
85	8 8 56.8	55 49 26	0.0120	1	13.80	0.03
86	8 9 43.1	46 8 33	0.0010	1	11.70	0.04
87	8 15 55.1	74 8 53	0.0100	1	13.40	0.03
88	8 24 18.0	55 52 34	0.0310	1	14.30	0.03
90	8 26 15.7	52 51 53	0.0150	1	13.90	0.03
100	8 54 29.8	66 39 47	0.0120	1	14.20	0.03
101	9 1 0.7	51 48 46	0.0160	1	13.60	0.02
102	9 8 18.1	46 50 33	0.0140	1	14.30	0.01
111	9 23 30.2	68 37 43	0.0130	1	13.90	0.04
114	9 26 36.8	56 4 20	0.0250	1	14.50	0.01
119	9 40 10.0	66 12 27	0.0100	1	14.10	0.03
122	9 43 14.5	73 11 50	0.0220	1	14.30	0.03
131	9 57 28.8	55 51 39	0.0040	1	13.80	0.01
133	9 57 52.0	72 21 53	0.0070	1	12.80	0.03
146	10 32 4.7	46 49 7	0.0110	1	14.10	0.00
149	10 34 38.9	64 31 32	0.0060	1	14.40	0.01
155	10 48 24.0	44 50 7	0.0060	1	13.20	0.00
156	10 50 10.6	50 33 0	0.0040	1	14.50	0.00
157	10 52 5.5	49 59 34	0.0050	1	14.00	0.00
158	10 56 1.6	61 47 46	0.0070	1	13.00	0.01
161	10 59 7.3	45 29 47	0.0200	1	13.40	0.00
169	11 23 52.9	59 25 47	0.0050	1	14.20	0.00
171	11 25 42.8	58 50 23	0.0100	1	11.80	0.00
171A	11 25 42.8	58 50 23	0.0110	1	12.70	0.00
175	11 29 37.5	62 47 0	0.0130	1	14.10	0.01
178	11 30 45.2	49 30 43	0.0010	1	13.90	0.00
179	11 30 51.8	62 9 53	0.0110	1	13.60	0.01
181	11 34 18.0	20 15 0	0.0200	1	13.90	0.00
185	11 38 36.0	47 58 13	0.0100	1	13.00	0.01
186	11 43 16.9	50 28 43	0.0030	1	13.20	0.00
188	11 44 53.9	56 14 57	0.0070	1	12.60	0.00
190	11 49 10.1	48 57 34	0.0030	1	13.10	0.00
195	12 0 3.1	64 39 20	0.0050	1	14.30	0.01
201	12 11 39.9	54 48 20	0.0090	1	13.00	0.00
207	12 22 48.0	54 46 53	0.0080	1	13.50	0.01
213	12 29 0.9	58 14 20	0.0100	1	13.20	0.00

TABLE 4.2.3 (CONTINUE.1)

MK <1>	A <2>	D <3>	Z <4>	R <5>	Mz <6>	EBV <7>
220	12 41 31.6	55 10 10	0.0170	1	14.10	0.00
249	13 15 8.6	57 48 0	0.0190	2	13.90	0.00
256	13 21 26.7	70 46 26	0.0110	1	13.20	0.02
271	13 39 47.2	55 55 19	0.0260	1	13.60	0.00
281	13 55 0.6	42 5 20	0.0080	1	12.50	0.00
286	14 18 46.5	71 48 46	0.0270	1	13.90	0.02
307	22 33 31.4	20 3 53	0.0190	1	13.70	0.05
313	22 59 31.8	15 41 47	0.0070	1	13.30	0.04
314	23 0 30.5	16 20 0	0.0080	1	14.00	0.04
319	23 16 10.3	24 57 27	0.0280	1	14.00	0.06
321	23 17 37.0	23 56 40	0.0330	1	13.50	0.06
323	23 17 55.0	27 2 26	0.0150	1	13.70	0.06
325	23 25 12.0	23 18 53	0.0120	1	12.70	0.05
326	23 25 36.0	23 15 17	0.0130	1	13.90	0.05
332	23 56 52.1	20 28 33	0.0090	1	12.70	0.03
333	23 58 52.7	31 9 20	0.0160	2	14.30	0.05
341	0 34 13.5	23 42 34	0.0170	1	13.30	0.01
353	1 0 35.0	22 4 26	0.0170	1	14.20	0.01
363	1 48 12.0	21 45 0	0.0100	1	13.90	0.02
368	2 30 1.4	20 25 27	0.0290	1	14.50	0.01
370	2 37 40.3	19 5 0	0.0030	1	13.50	0.09
394	9 16 7.0	26 28 50	0.0310	1	14.30	0.01
400	9 23 12.2	19 36 3	0.0080	1	14.40	0.01
401	9 27 19.5	29 45 33	0.0050	1	13.60	0.00
404	9 39 59.3	32 4 33	0.0040	1	12.00	0.00
409	9 46 44.6	32 26 53	0.0050	1	14.20	0.00
418	10 50 21.2	34 10 34	0.0060	1	13.20	0.00
430	11 48 28.0	55 21 20	0.0200	1	13.40	0.00
431	11 48 51.8	35 42 33	0.0100	2	14.30	0.00
432	11 55 31.1	28 9 20	0.0110	1	14.00	0.00
439	12 22 7.7	39 39 33	0.0040	1	12.30	0.00
442	12 44 59.4	35 37 27	0.0020	1	14.30	0.00
446	12 47 43.9	33 25 47	0.0240	1	14.20	0.00
449	13 9 12.0	36 32 47	0.0040	1	13.50	0.00
452	13 22 45.2	36 39 33	0.0170	1	14.00	0.00
470	14 20 24.8	37 20 54	0.0150	1	14.50	0.00
479	14 52 40.7	18 14 20	0.0210	1	13.90	0.01
480	15 4 44.4	42 50 0	0.0190	1	14.20	0.00
489	15 42 36.0	41 14 26	0.0320	1	14.20	0.00
491	15 49 41.4	43 34 0	0.0400	1	14.40	0.00
496	16 10 24.0	52 35 0	0.0290	1	14.00	0.01
518	21 56 9.3	11 47 53	0.0320	1	14.30	0.07
527	23 10 40.6	6 2 56	0.0120	1	14.50	0.02
531	23 21 22.3	9 23 35	0.0130	1	13.50	0.03
534	23 26 13.6	3 14 9	0.0180	1	13.20	0.03
538	23 33 41.2	1 52 42	0.0100	1	13.10	0.01
545	0 7 18.6	25 38 42	0.0160	1	12.50	0.03
547	0 17 53.5	0 33 20	0.0180	1	14.50	0.00

TABLE 4.2.3 (CONTINUE.2)

MK <1>	A <2>	D <3>	Z <4>	R <5>	Mz <6>	EBV <7>
555	0 43 32.2	-1-59-43	0.0140	1	12.90	0.00
562	1 9 13.1	0 55 43	0.0090	1	14.20	0.00
571	1 33 25.9	0 24 32	0.0180	1	14.10	0.00
575	1 45 52.8	12 21 51	0.0180	1	14.00	0.03
577	1 46 49.6	12 15 40	0.0420	1	14.20	0.03
582	1 55 31.2	2 50 40	0.0190	1	14.00	0.00
587	2 8 0.4	5 38 7	0.0150	1	14.50	0.01
589	2 11 8.7	3 52 8	0.0110	1	14.30	0.01
602	2 57 14.1	2 34 24	0.0100	1	13.20	0.06
649	12 34 2.2	26 28 34	0.0240	1	14.30	0.00
656	12 43 7.6	27 20 3	0.0230	1	13.70	0.00
665	13 59 30.2	34 4 1	0.0260	1	14.30	0.00
669	14 9 35.5	39 52 37	0.0180	2	13.90	0.00
703	8 56 11.5	6 29 17	0.0120	1	13.30	0.03
708	9 39 34.4	4 54 7	0.0060	1	14.00	0.02
710	9 52 10.2	9 30 32	0.0050	1	13.50	0.00
712	9 53 59.1	15 52 34	0.0150	1	14.30	0.00
718	10 9 35.4	5 10 16	0.0270	3	14.50	0.00
729	11 7 12.1	13 2 32	0.0420	1	14.20	0.00
731	11 10 3.7	9 19 44	0.0040	1	13.40	0.01
732	11 11 13.5	9 51 33	0.0290	3	13.90	0.01
736	11 25 21.3	29 47 12	0.0080	1	13.00	0.00
741	11 34 45.0	26 1 4	0.0110	3	14.50	0.00
743	11 35 37.8	12 23 20	0.0030	1	13.10	0.02
747	11 39 15.2	16 15 3	0.0020	1	14.50	0.02
752	11 50 6.9	2 1 43	0.0200	1	14.40	0.01
759	12 8 4.6	16 18 42	0.0070	1	12.50	0.02
761	12 9 55.0	29 25 38	0.0140	1	14.30	0.01
769	12 22 53.9	16 44 49	0.0050	1	12.30	0.01
773	12 30 38.9	32 22 7	0.0030	3	14.10	0.00
778	12 36 27.4	0 38 24	0.0230	2	14.40	0.01
781	12 51 19.6	9 58 49	0.0090	3	13.50	0.00
789	13 29 55.4	11 21 43	0.0320	1	14.50	0.00
799A	13 59 8.5	59 34 16	0.0110	1	12.70	0.01
800	13 59 35.6	10 10 12	0.0140	1	13.80	0.00
806	14 8 21.3	48 46 55	0.0060	2	14.50	0.00
809	14 20 10.1	13 56 40	0.0250	1	14.50	0.00
814	14 28 32.6	29 24 8	0.0130	3	14.40	0.01
829	14 48 55.1	35 46 36	0.0040	1	14.50	0.00
874	16 10 57.9	60 42 33	0.0140	6	14.50	0.01
991	1 21 56.5	31 54 20	0.0370	1	14.20	0.03
993	1 22 42.7	31 52 35	0.0150	2	14.00	0.01
1002	1 34 41.1	5 37 23	0.0110	2	13.50	0.02
1003	1 37 6.0	6 59 5	0.0100	4	14.40	0.02
1007	1 46 4.5	10 15 35	0.0170	1	14.20	0.03
1027	2 11 28.8	4 56 33	0.0300	1	14.40	0.03
1068	2 59 58.4	2 0 0	0.0170	2	14.00	0.06
1101	15 54 54.3	42 1 29	0.0340	1	14.30	0.00

TABLE 4.2.3 (CONTINUE.3)

MK <1>	A <2>	D <3>	Z <4>	R <5>	Mz <6>	EBV <7>
1134	23 44 27.1	29 10 52	0.0170	1	14.30	0.06
1230	9 14 10.5	25 38 21	0.0040	1	14.00	0.02
1233	9 31 36.6	0 27 55	0.0160	5	13.90	0.02
1236	9 47 19.9	0 51 0	0.0050	1	13.50	0.02
1237	9 47 30.3	44 33 55	0.0150	1	14.30	0.00
1260	10 36 55.9	5 22 9	0.0250	1	14.20	0.01
1261	10 41 19.2	-1 -1-55	0.0250	1	14.10	0.02
1264	10 46 31.3	7 10 37	0.0020	2	14.40	0.01
1267	10 50 28.5	4 53 52	0.0190	1	14.10	0.02
1288	11 15 53.5	23 44 33	0.0230	2	14.40	0.00
1301	11 33 10.8	35 36 44	0.0050	2	14.50	0.00
1304	11 39 38.5	0 36 42	0.0180	5	13.70	0.01
1308	11 51 38.5	0 24 53	0.0030	1	13.70	0.01
1325	12 23 55.3	9 17 54	0.0240	1	13.60	0.00
1326	12 24 14.0	8 11 44	0.0060	2	13.50	0.00
1346	13 19 9.0	38 47 59	0.0030	1	13.70	0.00
1365	13 52 6.0	15 17 21	0.0180	1	14.10	0.00
1418	9 37 9.8	48 33 53	0.0020	1	13.50	0.00
1425	9 44 33.5	54 14 50	0.0240	4	14.00	0.00
1443	11 13 6.6	41 51 49	0.0020	2	12.60	0.00
1466	12 5 37.4	3 9 22	0.0040	1	13.10	0.01
1478	13 23 30.8	59 52 18	0.0270	7	14.50	0.00
1479	13 33 42.7	51 52 9	0.0010	4	14.20	0.00
1485	13 51 14.6	40 36 32	0.0080	1	12.40	0.00

Entrence
<1> Markarian number
<2> right ascension
<3> declination
<4> redshift
<5> reference for redshift
<6> apparent blue magnitude
<7> extinction in our own galaxy

REFERENCES FOR REDSHIFTS

1 Palumbo, Tanzella-Nitti, and Vettolani 1983

2 Huchra et al 1983

3 Denisyuk, and Lipovetskii 1983

4 Markaryan, Lipovetskii, and Stepanyan 1983, 1984.

5 Dennefeld, and Sevre 1984.

6 Karachentsev 1981.

7 Markaryan et al 1985.

TABLE 4.2.4 OMITTED GALAXIES

MK <1>	A <2>			D <3>			Z <4>	R <5>	Mz <6>	EBV <7>
297	16	3	1.2	20	40	43	0.0160	1	14.10	0.03
389	8	29	15.4	22	44	0	0.0150	1	13.40	0.03
616	4	28	9.4	0	33	29	0.0120	1	14.10	0.06
626	8	42	26.3	37	7	1	0.0130	1	13.80	0.02
691	15	44	43.2	18	2	22	0.0110	1	13.20	0.02
839	15	0	32.6	83	43	16	0.0130	3	13.80	0.06
861	15	47	25.5	12	33	3	0.0150	3	14.50	0.01
900	21	27	27.5	2	11	39	0.0040	2	14.30	0.05
1104	16	4	3.7	41	28	40	0.0070	1	13.60	0.00
1224	9	1	48.9	14	47	40	0.0500	1	14.30	0.01
1496	15	52	24.5	16	45	49	0.0080	2	14.50	0.02

TABLE 4.2.5.A TULLY-FISHER DISTANCES OF NEARBY GALAXIES

NAME <1>	A <2>	D <3>	Z <4>	Mz <5>	D(Mpc) <6>	ref <7>	GROUP <8>
MK 401	9 27 19.5	29 45 33	0.005	13.60	76.033	6	*
MK1466	12 5 37.4	3 9 22	0.004	13.10	17.660	6	*
MK 86	8 9 43.1	46 8 33	0.001	11.70	19.861	6	*
MK1236	9 47 19.9	0 51 0	0.005	13.50	10.789	4	*
MK 133	9 57 52.0	72 21 53	0.007	12.80	58.479	5	*
MK 404	9 39 59.3	32 4 33	0.004	12.00	22.646	a,3	50
MK 409	9 46 44.6	32 26 53	0.005	14.20	22.646	a,3	50
MK 131	9 57 28.8	55 51 39	0.004	13.80	26.424	c,3	**
MK 33	10 29 22.2	54 39 23	0.005	13.20	20.091	a,2	94
MK 149	10 34 38.9	64 31 32	0.006	14.40	16.032	a,3	63
MK 35	10 42 16.4	56 13 20	0.004	12.90	20.091	a,2	94
MK 418	10 50 21.2	34 10 34	0.006	13.20	27.227	a,3	67
MK1443	11 13 6.6	41 51 49	0.002	12.60	16.406	a,3	75
MK 169	11 23 52.9	59 25 47	0.005	14.20	20.091	a,2	94
MK 178	11 30 45.2	49 30 43	0.001	13.90	20.091	a,2	94
MK1301	11 33 10.8	35 36 44	0.005	14.50	31.261	a,3	84
MK 186	11 43 16.9	50 28 43	0.003	13.20	20.091	a,2	94
MK 188	11 44 53.9	56 14 57	0.007	12.60	20.091	a,2	94
MK 190	11 49 10.1	48 57 34	0.003	13.10	20.091	a,2	94
MK 195	12 0 3.1	64 39 20	0.005	14.30	20.091	a,2	94
MK 759	12 8 4.6	16 18 42	0.007	12.50	19.999	b,2	106
MK 49	12 16 36.4	4 8 7	0.005	14.50	19.999	a,2	106
MK 439	12 22 7.7	39 39 33	0.004	12.30	20.091	a,2	94
MK 769	12 22 53.9	16 44 49	0.005	12.30	19.999	a,2	106
MK 52	12 23 8.9	0 51 0	0.007	12.40	19.999	a,2	106
MK1326	12 24 14.0	8 11 44	0.006	13.50	19.999	a,2	106
MK 773	12 30 38.9	32 22 7	0.003	14.10	20.091	a,2	94
MK 59	12 56 38.2	35 6 50	0.003	12.80	20.091	a,1	115
MK 449	13 9 12.0	36 32 47	0.004	13.50	20.091	a,1	115
MK1346	13 19 9.0	38 47 59	0.003	13.70	20.091	a,1	115
MK 806	14 8 21.3	48 46 55	0.006	14.50	38.994	a,3	135
MK 313	22 59 31.8	15 41 47	0.007	13.30	39.174	a,1	163
MK 171A	11 25 42.8	58 50 23	0.011	12.70	20.091	b,2	94
MK 171	11 25 42.8	58 50 23	0.010	11.80	20.091	b,2	94
MK 781	12 51 19.6	9 58 49	0.009	13.50	19.999	b,2	106

* separated galaxies.
** with in the same group of NGC3097.

notice: all the distances are calibrated according to D(Virgo)=20 Mpc.

Entrence

<1> Markarian number
<2> right ascension
<3> declination
<4> redshift
<5> apparent blue magnitude
<6> distance
<7> references for Tully-Fisher distance and membership of group.

References for group numbers

a Geller and Huchra (1983)

b Huchtmeier and Richter (1986)

c Turner and Gottii (1976)

References for distances

1 Giuricin et al (1986)

2 Aaronson et al (1979)

3 Aaronson et al (1982)

4 Bottineli et al (1985)

5 Bottineli et al (1986)

6 Bottineli et al (1984)

TABLE 4.2.5.B DISTANCES OF NEARBY GALAXIES

NAME <1>	A <2>	D <3>	Z <4>	Mz <5>	D(Mpc) <6>
MK1230	9 14 10.5	25 38 21	0.004	14.00	25.003
MK1418	9 37 9.8	48 33 53	0.002	13.50	9.057
MK 710	9 52 10.2	9 30 32	0.005	13.50	25.061
MK1264	10 46 31.3	7 10 37	0.002	14.40	10.814
MK 155	10 48 24.0	44 50 7	0.006	13.20	31.623
MK 156	10 50 10.6	50 33 0	0.004	14.50	23.550
MK 157	10 52 5.5	49 59 34	0.005	14.00	25.468
MK 158	10 56 1.6	61 47 46	0.007	13.00	34.834
MK 731	11 10 3.7	9 19 44	0.004	13.40	27.164
MK 743	11 35 37.8	12 23 20	0.003	13.10	20.606
MK 747	11 39 15.2	16 15 3	0.002	14.50	9.333
MK1308	11 51 38.5	0 24 53	0.003	13.70	10.423
MK 442	12 44 59.4	35 37 27	0.002	14.30	9.616
MK1479	13 33 42.7	51 52 9	0.001	14.20	4.753
MK1104	16 4 3.7	41 28 40	0.007	13.60	33.420
MK 370	2 37 40.3	19 5 0	0.003	13.50	11.885
MK 13	7 51 56.8	60 26 18	0.005	14.50	24.378
MK 708	9 39 34.4	4 54 7	0.006	14.00	32.359
MK 829*	14 48 55.1	35 46 36	0.004	14.50	28.774

* A member of Geller and Huchra's (1983) GROUP 161. The distance is derived from the mean radial velocity of the group.

TABLE 4.2.6 <V/Vm> TEST

m(B)	<V/Vm>	d	No
13.0	0.6183	0.0577	25
13.5	0.5835	0.0389	55
14.0	0.5182	0.0296	95
14.5	0.4910	0.0223	167
15.0	0.4517	0.0177	266
15.5	0.4309	0.0143	405

TABLE 4.2.7 OPTICAL LUMINOSITY FUNCTION OF MARKARIANS (TOTAL)

abs Mag <1>	Lg Y <2>	LgG <3>	Lg f <4>	err. <5>	Lg fII <6>	No. <7>
-14	-1.961	-2.002	0.041	0.963	0.027	1
-15	-2.772	-2.749	-0.023	0.694	-0.018	1
-16	-2.498	-2.464	-0.034	0.503	-0.006	4
-17	-2.869	-2.830	-0.039	0.368	-0.001	8
-18	-3.066	-3.020	-0.046	0.279	-0.001	19
-19	-3.772	-3.666	-0.056	0.225	-0.002	15
-20	-4.048	-3.975	-0.073	0.191	-0.004	30
-21	-4.491	-4.388	-0.103	0.180	-0.008	50
-22	-5.303	-5.116	-0.187	0.216	-0.044	33
-23	-6.846	-6.352	-0.494	0.496	-0.289	6

Entrance
<1> absolute blue magnitude
<2> logarithm of optical differetial luminosity function
<3> logarithm of uncorrected density
<4> logarithm of correcting factor
<5> fractional statistic error (error/Y)
<6> logarithm of second order correction
<7> number of objects in the bin

TABLE 4.2.8.A OPTICAL LUMINOSITY FUNCTION OF MARKARIANS (STELLAR)

abs Mag <1>	Lg Y <2>	LgG <3>	Lg f <4>	err. <5>	Lg fII <6>	No. <7>
-16	-2.674	-2.624	-0.050	0.560	-0.018	3
-17	-3.279	-3.222	-0.057	0.446	-0.005	3
-18	-3.356	-3.289	-0.067	0.368	-0.008	10
-19	-4.111	-4.030	-0.081	0.321	-0.009	7
-20	-4.378	-4.275	-0.103	0.300	-0.016	14
-21	-4.688	-4.547	-0.141	0.315	-0.033	35
-22	-5.577	-5.551	-0.226	0.410	-0.107	14
-23	-7.198	-6.751	-0.447	0.849	-0.355	3

TABLE 4.2.8.B OPTICAL LUMINOSITY FUNCTION OF MARKARIANS (DIFFUSE)

abs Mag <1>	Lg Y <2>	LgG <3>	Lg f <4>	err. <5>	Lg fII <6>	No. <7>
-14	-1.961	-2.002	0.041	1.320	0.063	1
-15	-2.774	-2.749	-0.025	0.995	-0.043	1
-16						0
-17	-3.098	-3.056	-0.042	0.542	-0.004	5
-18	-3.512	-3.463	-0.048	0.419	-0.004	7
-19	-3.972	-3.912	-0.060	0.337	-0.005	8
-20	-4.354	-4.277	-0.077	0.291	-0.009	16
-21	-5.009	-4.901	-0.108	0.279	-0.021	15
-22	-5.555	-5.370	-0.185	0.330	-0.088	17
-23	-7.006	-6.573	-0.433	0.667	-0.392	3

TABLE 4.2.9 INFRARED DATA

MK <1>	LOG(D(Mpc) <2>	ABS.MAG <3>	F60(JY) <4>	FIR(E-14WM-2) <5>
12	1.92428	-22.04064	3.18000	28.45282
13	1.38700	-17.55500	< 0.48000	< 4.24948
14	1.81954	-19.81697	1.07000	8.14703
18	1.81954	-19.91697	2.07000	15.83933
25	1.73239	-19.50121	1.30000	9.43866
33	1.30300	-18.31500	4.73000	32.98692
35	1.30300	-18.61500	5.13000	37.05421
49	1.30100	-17.00500	0.74000	< 5.49839
52	1.30100	-19.14500	4.58000	33.50290
59	1.30300	-18.71500	1.82000	13.20278
84	2.07918	-21.91515	1.35000	11.47797
85	1.85733	-20.60591	< 0.60000	< 5.01227
86	1.29800	-19.95000	3.15000	27.19143
87	1.77815	-20.61000	1.31000	12.83272
88	2.26951	-22.16681	1.27000	10.93667
90	1.95424	-20.99046	0.87000	8.36249
100	1.85733	-20.20591	1.39000	11.37062
101	1.98227	-21.39060	0.93000	9.05197
102	1.92428	-20.36064	0.69000	< 6.36967
111	1.89209	-20.71972	2.82000	24.44828
114	2.17609	-21.41970	1.52000	13.08182
119	1.77815	-19.91000	2.17000	18.16026
122	2.12057	-21.42212	1.07000	10.43393
131	1.42200	-18.35000	< 0.60000	< 5.01227
133	1.76700	-21.15500	3.02000	25.00772
146	1.81954	-19.99696	0.89000	6.79682
149	1.20500	-16.66500	< 0.60000	< 5.01227
155	1.50000	-19.30000	< 0.60000	< 5.01227
156	1.37200	-17.36000	< 0.60000	< 5.01227
157	1.40600	-18.03000	0.62000	5.48024
158	1.54200	-19.75000	8.40000	63.20538
161	2.07918	-21.99515	2.46000	19.44205
169	1.30300	-17.31500	3.59000	26.16176
171	1.30300	-19.71500	70.30000	480.47831
171A	1.30300	-18.81500	35.10000	240.23916
175	1.89209	-20.39972	< 0.60000	< 5.01227
178	1.30300	-17.61500	< 0.60000	< 5.01227
179	1.81954	-20.53696	0.99000	9.23114
181	2.07918	-21.49515	1.95000	17.46549
185	1.77815	-20.93000	2.47000	22.40141
186	1.30300	-18.31500	1.17000	10.26005
188	1.30300	-18.91500	4.76000	43.92511
190	1.30300	-18.41500	2.65000	22.80663
195	1.30300	-17.25500	1.79000	13.49120
201	1.73239	-20.66121	22.50000	157.34250

TABLE 4.2.9 (CONTINUE.1)

MK <1>	LOG(D(Mpc) <2>	ABS.MAG <3>	F60(JY) <4>	FIR(E-14WM-2) <5>
207	1.68124	-19.94545	2.21000	18.37420
213	1.77815	-20.69000	3.89000	31.34792
220	2.00860	-20.94224	1.82000	14.52578
249	2.05690	-21.38377	< 1.50000	< 12.53070
256	1.81954	-20.97696	2.87000	24.29519
271	2.19312	-22.36487	1.50000	15.25230
281	1.68124	-20.90545	5.23000	49.31653
286	2.20952	-22.22682	4.40000	33.51348
307	2.05690	-21.78377	1.83000	16.91815
313	1.59300	-19.82500	3.12000	27.61214
314	1.68124	-19.56545	1.29000	9.21980
319	2.22531	-22.36579	4.21000	33.81550
321	2.29667	-23.22257	2.67000	24.60515
323	1.95424	-21.31046	2.98000	30.35037
325	1.85733	-21.78591	5.18000	37.94062
326	1.89209	-20.75972	3.85000	29.92437
332	1.73239	-21.08121	4.98000	42.57868
333	1.98227	-20.81060	< 1.50000	< 12.53070
341	2.00860	-21.78225	0.85000	10.64637
353	2.00860	-20.88225	3.89000	30.23282
363	1.77815	-20.07000	2.40000	18.62028
368	2.24055	-21.74199	0.71000	6.08920
370	1.07500	-17.23500	1.12000	10.96124
394	2.26951	-22.08681	1.28000	9.56794
400	1.68124	-19.04545	1.22000	10.33376
401	1.88100	-20.80500	2.49000	19.07804
404	1.35500	-19.77500	11.66000	100.78009
409	1.35500	-17.57500	< 0.60000	< 5.01227
418	1.43500	-18.97500	1.74000	14.19239
430	2.07918	-21.99515	0.83000	7.18465
432	1.81954	-20.09696	3.58000	29.62840
439	1.30300	-19.21500	5.91000	49.91074
442	0.98300	-15.61500	< 1.50000	< 12.53070
446	2.15836	-21.59106	1.45000	11.79549
449	1.30300	-18.01500	2.27000	18.68567
452	2.00860	-21.04224	< 1.50000	< 12.53070
470	1.95424	-20.27046	< 1.50000	< 12.53070
479	2.10037	-21.64110	1.65000	14.49063
480	2.05690	-21.08377	1.80000	14.50386
489	2.28330	-22.21575	1.50000	< 16.57530
491	2.38021	-22.50030	< 0.60000	< 5.01227
496	2.24055	-22.24199	6.43000	49.49797
518	2.28330	-22.39575	2.70000	20.72574
527	1.85733	-19.86591	4.37000	34.89809

TABLE 4.2.9 (CONTINUE.2)

MK <1>	LOG(D(Mpc) <2>	ABS.MAG <3>	F60(JY) <4>	FIR(E-14WM-2) <5>
531	1.89209	-21.07972	4.71000	36.08350
534	2.03342	-22.08636	7.29000	53.55920
538	1.77815	-20.83000	11.07000	74.61833
545	1.98227	-22.53060	8.98000	73.55578
547	2.03342	-20.66636	0.64000	5.02967
555	1.92428	-21.72064	3.89000	35.69492
562	1.73239	-19.46121	< 1.50000	< 12.53070
571	2.03342	-21.06636	1.48000	12.41428
575	2.03342	-21.28636	2.74000	24.53069
577	2.40140	-22.92625	< 1.50000	< 12.53070
582	2.05690	-21.28377	4.94000	39.35963
587	1.95424	-20.31046	0.91000	7.66924
589	1.81954	-19.83697	2.66000	19.39669
602	1.77815	-20.93000	3.55000	27.85671
649	2.15836	-21.49106	< 1.50000	< 12.53070
656	2.13988	-21.99864	< 1.50000	< 12.53070
665	2.19312	-21.66487	0.67000	6.65015
669	2.03342	-21.26636	< 1.50000	< 12.53070
703	1.85733	-21.10591	3.95000	32.03739
708	1.51000	-18.63000	5.37000	41.28629
710	1.39900	-18.49500	2.66000	20.87089
712	1.95424	-20.47046	0.84000	7.04441
718	2.20952	-21.54682	1.31000	12.20902
731	1.43400	-18.81000	2.99000	23.23604
732	2.24055	-22.34199	1.91000	15.53164
743	1.31400	-18.55000	1.48000	10.56208
747	0.97000	-15.43000	< 1.50000	< 12.53070
752	2.07918	-21.03515	0.71000	6.33490
759	1.30100	-19.08500	4.13000	37.52671
761	1.92428	-20.36064	5.33000	46.28875
769	1.30100	-19.24500	8.53000	64.23618
773	1.30300	-17.41500	0.60000	< 6.81912
778	2.13988	-21.33864	< 1.50000	< 12.53070
781	1.30100	-18.00500	1.82000	16.71818
789	2.28330	-21.91575	3.79000	28.61120
799A	1.81954	-21.43697	10.64000	89.38037
800	1.92428	-20.82064	2.52000	19.96142
806	1.59100	-18.45500	< 0.60000	< 5.01227
809	2.17609	-21.37970	1.80000	14.99526
814	1.89209	-20.09972	1.53000	12.28009
829	1.45900	-17.79500	0.71000	6.10810
874	1.92428	-20.16064	0.47000	< 4.69211
991	2.34635	-22.65101	1.42000	12.06500
993	1.95424	-20.81046	< 0.40000	< 4.27519
1002	1.81954	-20.67696	4.85000	35.61327
1003	1.77815	-19.57000	0.59000	5.25836
1007	2.00860	-20.96225	< 1.50000	< 12.53070
1027	2.25527	-21.99561	5.28000	41.20654
1068	2.00860	-21.28224	1.16000	10.53259

TABLE 4.2.9 (CONTINUE.3)

MK <1>	LOG(D(Mpc) <2>	ABS.MAG <3>	F60(JY) <4>	FIR(E-14WM-2) <5>
1101	2.30963	-22.24739	1.86000	15.30673
1134	2.00860	-20.98224	4.76000	41.99731
1230	1.39800	-18.07000	1.12000	8.39084
1233	1.98227	-21.09060	2.79000	22.33640
1236	1.03300	-16.74500	2.28000	20.28424
1237	1.95424	-20.47046	< 0.60000	< 5.01227
1304	2.03342	-21.50636	3.81000	26.78092
1308	1.01800	-16.43000	< 1.50000	< 12.53070
1325	2.15836	-22.19106	< 1.50000	< 12.53070
1326	1.30100	-18.00500	0.97000	10.00301
1346	1.30300	-17.81500	0.88000	7.27726
1365	2.03342	-21.06636	3.84000	29.27081
1418	0.95700	-16.28500	0.56000	5.01757
1425	2.15836	-21.79106	1.00000	8.97750
1443	1.21500	-18.47500	1.22000	11.05196
1466	1.24700	-18.17500	5.88000	48.70606
1478	2.20952	-21.54682	0.98000	8.52088
1479	0.67700	-14.18500	< 1.50000	< 12.53070
1485	1.68124	-21.00545	2.24000	26.51519

Notice

The 10 galaxies which are in our optical sample but out of the region covered by the IRAS survey are the following:
171, 431, 729, 736, 741, 1260, 1261, 1264, 1267, 1288, 1301.

TABLE 4.2.10 MONOCHRAMATIC IR (60μm) LUMINOSITY FUNCTION OF MARKARIAN GALAXIES

Lg L(60) <1>	IR(60) LF <2>	err. <3>
28.75	2.82E-2	2.07E-2
29.25	5.24E-3	2.90E-3
29.75	1.93E-3	8.07E-4
30.25	6.89E-4	2.37E-4
30.75	2.17E-4	7.62E-5
31.25	1.09E-4	3.52E-5
31.75	2.95E-5	1.02E-5
32.25	1.70E-6	7.14E-7

Entrence
<1> logarithm of 60 microns luminosity (erg/sec/Hz)
<2> IR (60microns) luminosity function
<3> statistical error

TABLE 4.2.11 INTEGRATED IR (42.5μ--122.5μ) LUMINOSITY FUNCTION OF MARKARIAN GALAXIES

Lg Lir <1>	IR LF <2>	err. <3>
8.35	5.08E-3	2.97E-3
8.85	1.58E-3	1.19E-3
9.35	1.32E-3	4.67E-4
9.85	2.29E-4	8.50E-5
10.35	1.59E-4	4.21E-5
10.85	5.46E-5	1.41E-5
11.35	5.54E-6	2.20E-6
11.85	1.04E-7	1.04E-7

Entrence
<1> logarithm of integrated IR luminosity (L⊙)
<2> integrated IR luminosity function
<3> statistical error

TABLE 4.2.12 <V/Vm> DISTRIBUTION

Mb <1>	<V/Vm> <2>	d <3>	No <4>
-15	1.000	0.288	1
-16	0.553	0.144	4
-17	0.671	0.102	8
-18	0.448	0.066	19
-19	0.220	0.075	15
-20	0.606	0.053	30
-21	0.453	0.041	50
-22	0.514	0.050	33
-23	0.528	0.118	6

Notice: All <V/Vm>s are calculated with mb(lim)=14.5.